

Transition State Mimetics of the *Plasmodium* Export Element Are Potent Inhibitors of Plasmepsin V from *P. falciparum* and *P. vivax*

Brad E. Sleebs,^{*,†,‡} Michelle Gazdik,^{†,‡} Matthew T. O'Neill,^{†,‡} Pravin Rajasekaran,^{†,‡} Sash Lopaticki,^{†,‡} Kurt Lackovic,^{†,‡} Kym Lowes,^{†,‡} Brian J. Smith,[§] Alan F. Cowman,^{†,‡} and Justin A. Boddey^{†,‡}

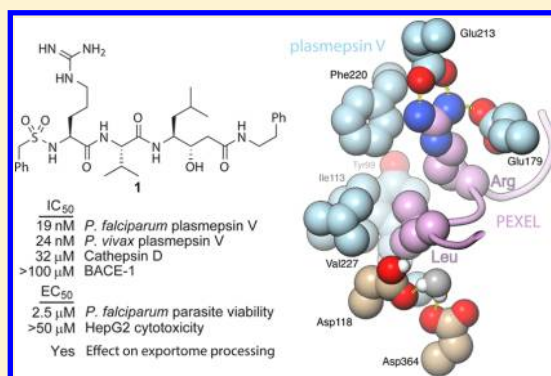
[†]The Walter and Eliza Hall Institute of Medical Research, 1G Royal Parade, Parkville 3052, Victoria, Australia

[‡]Department of Medical Biology, The University of Melbourne, Parkville 3010, Victoria, Australia

[§]Department of Chemistry, La Trobe Institute for Molecular Science, La Trobe University, Melbourne 3086, Victoria, Australia

S Supporting Information

ABSTRACT: Following erythrocyte invasion, malaria parasites export a catalogue of remodeling proteins into the infected cell that enable parasite development in the human host. Export is dependent on the activity of the aspartyl protease, plasmepsin V (PMV), which cleaves proteins within the *Plasmodium* export element (PEXEL; RxL↓xE/Q/D) in the parasite's endoplasmic reticulum. Here, we generated transition state mimetics of the native PEXEL substrate that potently inhibit PMV isolated from *Plasmodium falciparum* and *Plasmodium vivax*. Through optimization, we identified that the activity of the mimetics was completely dependent on the presence of P₁ Leu and P₃ Arg. Treatment of *P. falciparum*-infected erythrocytes with a set of optimized mimetics impaired PEXEL processing and killed the parasites. The striking effect of the compounds provides a clearer understanding of the accessibility of the PMV active site and reaffirms the enzyme as an attractive target for the design of future antimalarials.



■ INTRODUCTION

Malaria is caused by infection with protozoan parasites of the genus *Plasmodium*. Each year these parasites cause several hundred million infections and over 650 000 deaths, predominantly of children and pregnant women.¹ The two most lethal forms of malaria are caused by infection with *Plasmodium falciparum*, which is hyperendemic in Africa and the most deadly parasite, or *P. vivax*, which is responsible for recrudescence infection via activation of dormant liver-stage hypnozoites that replenish the clinical blood stage of infection.²

Following invasion of an erythrocyte, malaria parasites reside within a parasitophorous vacuole. To survive within the host cell, parasites export proteins beyond the parasite membrane and the parasitophorous vacuole membrane into the erythrocyte and onto its surface. In many cases, export requires the *Plasmodium* export element (PEXEL; RxLx↓E/Q/D)³ or vacuolar transport signal (VTS),⁴ which is located in the N-terminus of over 450 *P. falciparum* proteins. This represents a predicted "exportome" of almost 9% of all proteins,^{5,6} 20%, or more, of which are predicted to be essential.⁷ PEXEL-containing proteins are cleaved at the carboxy terminal of the PEXEL Leu residue (RxL↓) in the parasite endoplasmic reticulum (ER)⁸ by the ER-resident aspartyl protease, plasmepsin V (PMV).^{10,13} Cleavage of PEXEL cargo by PMV requires the conserved Arg and Leu residues⁹ and occurs within seconds of cotranslational insertion into the ER,¹¹ indicating

that PMV acts as the first step for export of PEXEL-containing proteins.

The PEXEL motif and PMV are conserved in all *Plasmodium* spp. *Plasmodium vivax* contains a PMV orthologue and it is functionally conserved,¹¹ as well as many PEXEL-containing proteins, some of which have been shown to be exported to the host cell.^{3,12} This strongly suggests that the function of PMV is to cleave the PEXEL motif for export across *Plasmodium* spp. The PMV gene could not be deleted from *P. falciparum* or *Plasmodium berghei*, consistent with a role that is essential for parasite survival.^{10,13,14} PMV is a phylogenetically unique aspartyl protease^{10,13,14} that shares little conservation with human proteases, suggesting it may be a promising candidate for antimalarial intervention.¹⁵

Chloroquine or artemisinin combination therapies have been used to successfully treat millions of malaria infections; however, the emergence and spread of resistance to these antimalarial agents highlights the urgent need for the development of new antimalarial therapies against novel targets.^{10–16} A clear benefit would be gained from targeting proteins that are shared between multiple *Plasmodium* spp. that infect humans.

Historically, aspartyl proteases have been targeted via transition state (TS) peptidomimetics that outcompete the

Received: May 23, 2014

Published: August 28, 2014

natural substrate to block protease function. A classic transition state mimetic is statine, which possesses a hydroxyl functionality that mimics the TS of amide bond proteolysis, inhibiting proteolysis. Statine has been utilized previously to inhibit the digestive vacuole plasmepsins I–IV of the malaria parasite.^{17–20} These mimetics demonstrated potent inhibition of the plasmepsins I–IV; however, they displayed weak activity against parasites in culture, presumably due to the redundancy, and nonessential nature, of the digestive vacuole plasmepsins.²¹ Targeting aspartic proteases with TS mimetics has generated compounds that have aided in the study of biological mechanisms²² as well as being clinically relevant, for example, inhibitors of renin (aliskiren) and HIV protease.^{23–25}

Recently, we described the use of statine to develop a potent inhibitor of PMV, called WEHI-916 (herein, compound 1), from *P. falciparum* and *P. vivax*, which perturbs protein export to the *P. falciparum*-infected erythrocyte and kills the parasite (Figure 2).¹¹

Here, we describe the use of statine to develop a repertoire of PEXEL mimetic compounds, some of which display potent inhibition of PMV from *P. falciparum* and *P. vivax*, and the steps taken to arrive at 1. We used the mimetics to define regions of the substrate that are essential to, or dispensable for, inhibition of PMV in vitro and in *P. falciparum*-infected erythrocytes and for parasite death. This new information will guide the development of future inhibitors that block this enzyme.

RESULTS AND DISCUSSION

The aim of the current study was to derive one or more TS mimetics that potently inhibit PMV. While the polar nature of peptide mimetics can be detrimental to target activity in cells and reduce cell permeability, we chose to generate compounds that directly mimic the natural PEXEL substrate (Figure 1) to reduce the likelihood of parasite resistance to the inhibitors and to further investigate accessibility to the active site of PMV from *P. falciparum* and *P. vivax*.^{5,9}

Molecular Modeling of PMV in Complex with Substrates. Compound design was assisted by generating a homology model of PfPMV in complex with the PEXEL motif from knob-associated histidine-rich protein (KAHRP) and a statine derivative of the PEXEL peptide (Arg-Ala-Sta(isobutyl)-Ala-Gln). The model indicated that the catalytic acid (Asp118)

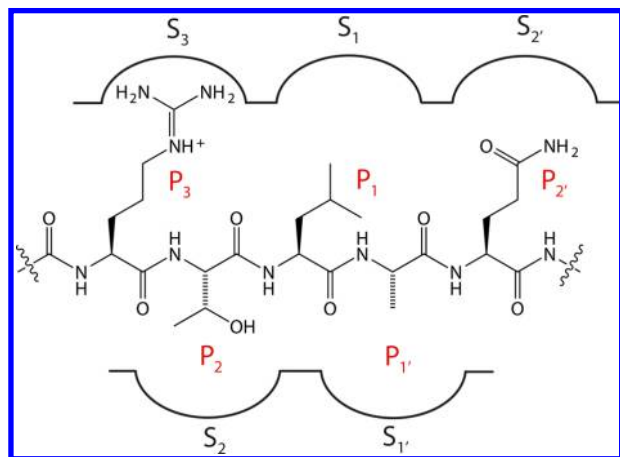


Figure 1. KAHRP PEXEL residues (P_3 – P_2') and the associated binding pockets of PMV (S_3 – S_2').

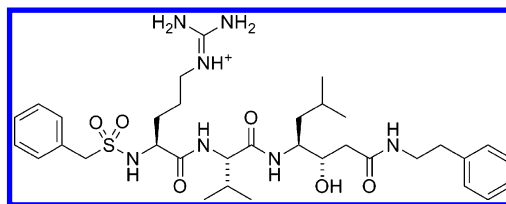


Figure 2. Structure of the previously described plasmepsin V inhibitor 1 (WEHI-916).¹¹

of PMV forms hydrogen bonds with the carbonyl of the scissile bond of the PEXEL and a water molecule; the water molecule, in turn, forms a hydrogen bond with the catalytic base (Figure 3). In these models, the S_3 pocket of PMV is lined by the aspartates Glu179 and Glu213, which form salt bridges with the guanidine side chain of the PEXEL P_3 Arg, which also forms salt bridges with the side chains of Tyr177 and Phe220 of PMV. The side chain carboxylate of Glu197 is held in position by a hydrogen bond with the backbone amide of the PEXEL “x” residue (RxL). The S_1 pocket of PMV is lined by the side chains of Tyr99, Ile113, Tyr177, Phe220, Val227, and Gly367 (Figure 3). The P_2 Thr of the KAHRP PEXEL makes nonspecific hydrophobic contact with residues Cys178 and Glu179 of the molecular “flap” of PMV, while the P_1' Lys of the KAHRP PEXEL makes no direct contact with PMV. The P_2' Gln forms a single hydrogen bond with Ser76 of PMV. The model suggests an intimate association of the PEXEL Arg and Leu with the binding site residues of PMV, as does the peptide backbone flanking the scissile bond, but few other critical interactions.

Compound Synthesis. In general, TS mimetics were synthesized using conventional solution phase peptide coupling methods (Scheme 1). The synthesis of the early P_1'/P_2' analogues started from the protected ornithine 8 that was coupled with alanine ethyl ester. The *N*-Cbz group of the resulting dipeptide was deprotected under hydrogenolytic conditions and *N*-acylated with acetic anhydride to give the *N*-acetamide 9. The *N*-Boc protection was then removed using acidic media and reacted with *N,N*-bis-Boc guanyl pyrazole to install the protected guanidine. The ester was subsequently removed by hydrolysis to obtain the acid 10 ready for coupling of the prepared statine amides 4–6. Finally, deprotection of the diBoc guanidine functionality gave 11–13.

The exploration of the P_3 position again utilized the protected ornithine 8 as a starting material and additionally protected lysine 14 (Scheme 2). The synthons 8 and 14 were then coupled to alanine ethyl ester and hydrolysis of the resulting gave 15 and 16, respectively. Boc deprotection of 15 and 16 then afforded the ornithine and lysine variants, 17 and 18, respectively. These analogues were further utilized synthetically to access both the arginine and homoarginine derivatives, 19 and 20, via reaction with *N,N*-bis-Boc guanyl pyrazole, followed by Boc deprotection.

The synthesis of P_1 variants began with the commercially available Boc protected synthons 21–24 that were coupled with cyclohexylamine and then Boc deprotected to afford 25–28, respectively. The resulting amides 25–28 were subsequently coupled with Cbz-Arg(*N,N*-diBoc)-Ala-OH to give 29–32 and further Boc deprotected to afford the P_1 derivatives 33–36 (Scheme 3). The P_2 derivatives required incorporation of Val, Leu, Ile, or Phe into the P_2 position; synthesis of these derivatives was performed by coupling the corresponding amino acid ester with the protected ornithine 8 to form the

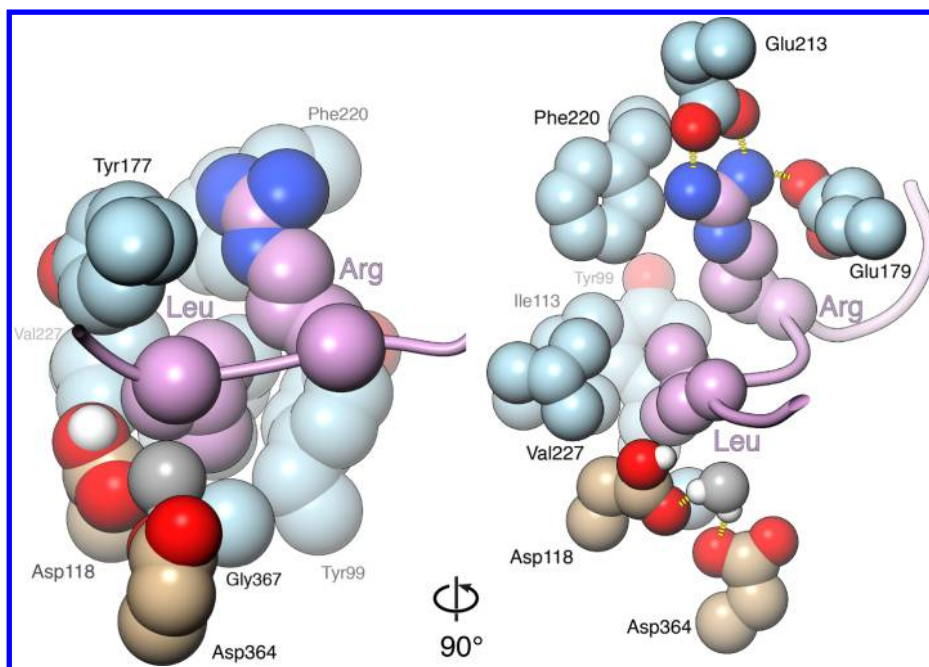
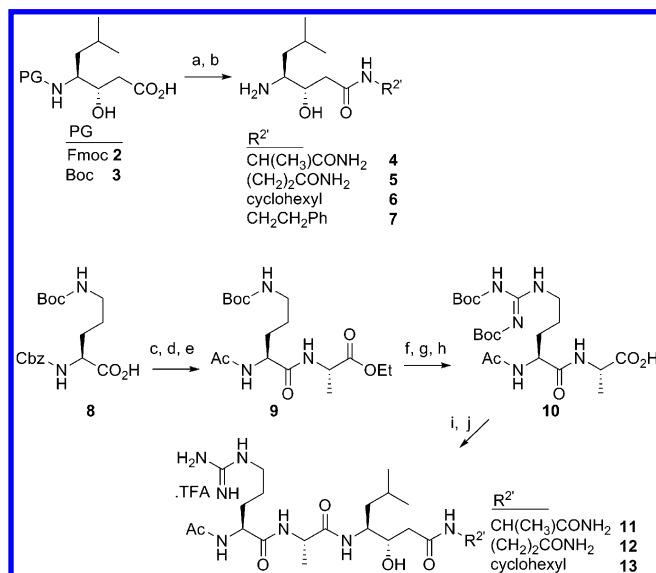


Figure 3. Modeling studies highlight the important binding interactions of PMV (cyan and tan) with the KAHRP PEXEL (violet). A space filling representation showing the arrangement of catalytic acid (Asp118), base (Asp364) (tan), and water molecule (gray). From the modeling studies, the P₃ Arg of the PEXEL motif forms salt bridges with Glu179 and Glu213 and packs against the hydrophobic side chain of Phe220 in the S₃ pocket of PMV. The P₁ Leu of the PEXEL packs tightly in the S₁ pocket of PMV formed by the side chains of residues Tyr99, Ile113, Phe220, and Val 227.

Scheme 1. Synthesis of P₁/P₂ Analogues^a

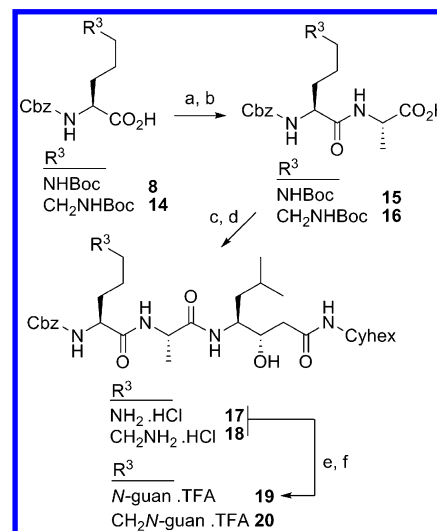


^aReagents and conditions: (a) HBTU, Et₃N, DMF, R²-NH₂; (b) For Fmoc, piperidine, DMF; for Boc, 4 N HCl dioxane; (c) CDI, Et₃N, ethyl alaninate.HCl, THF; (d) Pd/C, H₂, EtOAc; (e) Ac₂O, Et₃N; (f) 4 N HCl dioxane; (g) *N,N'*-bis-Boc-1-guanylpyrazole, Et₃N, DCM; (h) LiOH, THF/H₂O; (i) 4–6, HBTU, Et₃N, DMF; (j) TFA, DCM.

dipeptides 37–41 after hydrolysis of the ester functionality with LiOH. Coupling of 37–41 with the statine Cyhex amide 6 gave the tripeptides 42–45. The Boc protected ornithine residue of the tripeptides 42–45 was then converted to the corresponding arginine residue over three synthetic steps, resulting in the desired P₂ analogues 46–49 (Scheme 4).

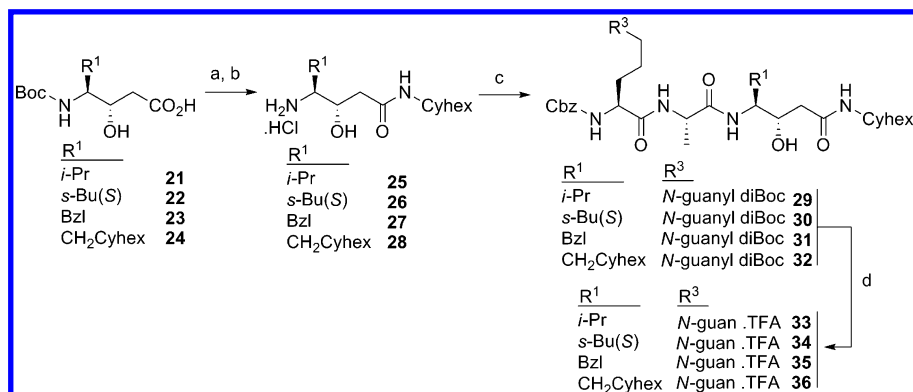
The key carboxylic acid 51 was synthesized to generate probes to investigate the S₁/S₂' pockets. Compound 51 was

Scheme 2. Synthesis of P₃ Analogues^a

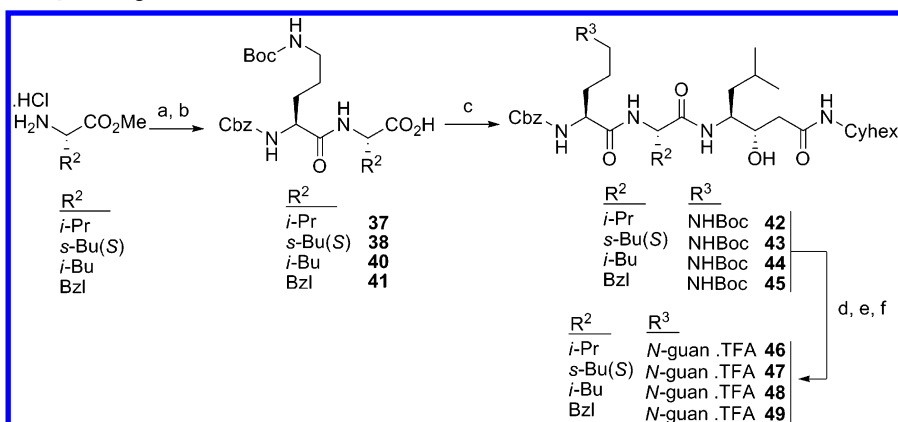


^aReagents and conditions: (a) CDI, Et₃N, ethyl alaninate.HCl, THF; (b) LiOH, THF/H₂O; (c) 6, HBTU, Et₃N, DMF; (d) 4 N HCl dioxane; (e) *N,N'*-bis-Boc-1-guanylpyrazole, Et₃N, DCM; (f) TFA, DCM.

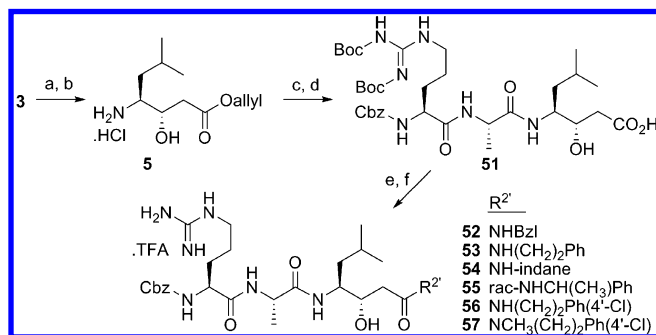
obtained by coupling the allyl ester of statine 50 with Cbz-Arg(*N,N*-diBoc)-Ala-OH 90, followed by ester hydrolysis (Scheme 5). 51 was then utilized in a parallel chemistry study that involved EDCI coupling reactions with a selection of hydrophobic amines followed by Boc deprotection to generate an array of amides A1–D6 (parallel set 1; Supporting Information, Scheme S1 and Table S1). After evaluation of the array (A1–D6) at 1 μM against *P. falciparum* PMV, the amides 52–57 were resynthesized to allow IC₅₀ values to be obtained (Scheme 5).

Scheme 3. Synthesis of P₁ Analogues^a

^aReagents and conditions: (a) HBTU, Et₃N, DMF, NH₂Cyhex; (b) 4 N HCl dioxane; (c) Cbz-Arg(*N,N*-diBoc)-Ala-OH **90**, HBTU, Et₃N, DMF; (d) TFA, DCM.

Scheme 4. Synthesis of P₂ Analogues^a

^aReagents and conditions: (a) **8**, HBTU, Et₃N, DMF; (b) LiOH, THF/H₂O; (c) **6**, HBTU, Et₃N, DMF; (d) 4 N HCl dioxane; (e) *N,N'*-bis-Boc-1-guanylpiprazole, Et₃N, DCM; (f) TFA, DCM.

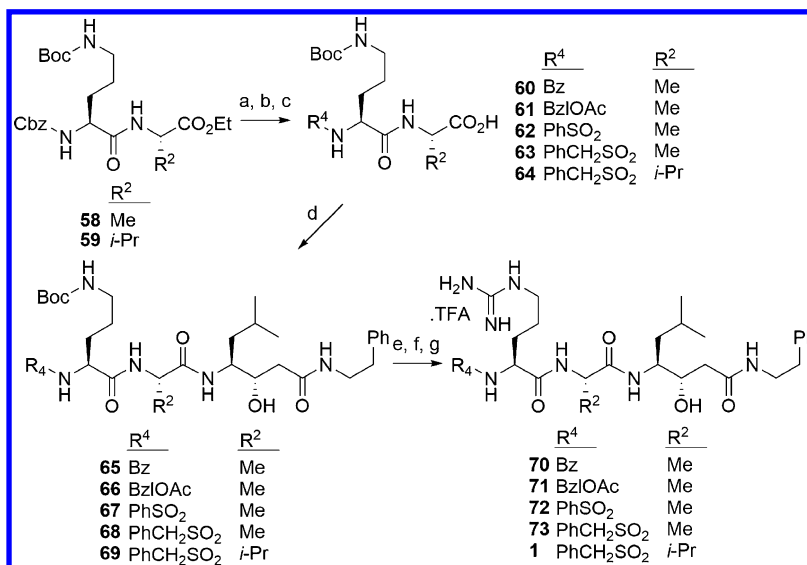
Scheme 5. Synthesis of P₁'/P₂' Analogues^a

^aReagents and conditions: (a) allyl-Br, K₂CO₃, DMF; (b) 4 N HCl dioxane; (c) Cbz-Arg(*N,N*-diBoc)-Ala-OH **90**, HBTU, Et₃N, DMF; (d) LiOH, THF/H₂O; (e) R^{2'}NH₂, HBTU, Et₃N, DMF; (f) TFA, DCM.

Parallel chemistry was also used to initially assess the changes to the P₄ region of the mimetics. This exploited the protected synthon **126** to perform a series of acylations using a small set of isocyanates, acid and sulfonyl chlorides (Supporting Information, Table S2). The acylated products were then deprotected using TFA (parallel set 2; Supporting Information, Scheme S2). The array (**11**–**15**) was evaluated at 1 μM against *P. falciparum* PMV. From this parallel study, a small cohort of

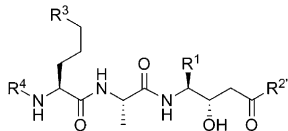
analogues (**70**–**73**) was selected for resynthesis to allow IC₅₀ determination. The resynthesis of analogues **70**–**73** utilized the protected dipeptide **58**. The Cbz functionality of **58** was deprotected by hydrogenolysis, and the product was acylated with the appropriate acyl or sulfonyl halide, followed by ester hydrolysis, to afford the carboxylic acids **60**–**63**. The acylated products **60**–**63** were then coupled with Sta amide **7** to give the tripeptides **65**–**68**. The tripeptides **65**–**68** were then converted to the corresponding P₄ variants **70**–**73** over three synthetic steps. Compound **1** was produced in a similar manner to **73**, with Ala replaced by Val in the P₂ position (Scheme 6).

Compound Evaluation. Compounds were evaluated using a fluorogenic PEXEL cleavage assay (see Experimental Section) described previously.^{5,11,13} Reactions comprised of a fluorescent peptide of nine amino acids containing the PEXEL sequence (RTLAQ) from KAHRP in PMV digest buffer and PMV-agarose (anti-HA-agarose bound to HA-tagged *P. falciparum* PMV or *P. vivax* PMV, both purified from *P. falciparum*; PfPMV or PvPMV, respectively). The purity and specificity of Pf or Pv PMV-agarose for the KAHRP PEXEL peptide has been well characterized and described previously.^{5,11,13} A PEXEL mutant form of the KAHRP peptide (RL > A) was used as a control. IC₅₀ values were determined using PfPMV in a nine-point compound dilution series. Only limited quantities of PvPMV were available, and compound inhibition was therefore assessed at 1 μM; this allowed a direct comparison of

Scheme 6. Synthesis of P₄ Analogues^a

^aReagents and conditions: (a) Pd/C, H₂, EtOAc; (b) R⁴-Cl, Et₃N, DCM; (c) LiOH, THF/H₂O; (d) 7, HBTU, Et₃N, DMF; (e) 4 N HCl dioxane; (f) *N,N'*-bis-Boc-1-guanylpiprazole, Et₃N, DCM; (g) TFA, DCM.

Table 1. Protease Activity of TS Mimetics, Probing the P₄, P₃, P₁, and P₁'/P₂' Moieties

Cmpd					Protease inhibition			cLogP ^d
	R ⁴	R ³	R ¹	R ^{2'}	PfPMV (±SEM) ^a	cathepsin D (±SEM) ^b	BACE-1 ^c	
74	Ac	<i>N</i> -guan	<i>i</i> -Bu	Gln-NH ₂	0.556 (0.116)	>100	>100	-4.9
11	Ac	<i>N</i> -guan	<i>i</i> -Bu	Ala-NH ₂	0.613 (0.299)	>100	>100	-3.8
12	Ac	<i>N</i> -guan	<i>i</i> -Bu	NHPrCONH ₂	0.865 (0.264)	>100	>100	-3.8
13	Ac	<i>N</i> -guan	<i>i</i> -Bu	NHCyhex	0.967 (0.410)	>100	>100	-1.2
17	Cbz	NH ₂	<i>i</i> -Bu	NHCyhex	>20	>100	>100	1.9
18	Cbz	CH ₂ NH ₂	<i>i</i> -Bu	NHCyhex	>20	>100	>100	2.3
19	Cbz	<i>N</i> -guan	<i>i</i> -Bu	NHCyhex	0.614 (0.143)	>100	>100	1.2
20	Cbz	CH ₂ <i>N</i> -guan	<i>i</i> -Bu	NHCyhex	>20	nd	nd	1.6
75	Cbz	(CH ₂) ₁ Ph	<i>i</i> -Bu	NHCyhex	>20	0.043 (0.016)	>100	4.5
33	Cbz	<i>N</i> -guan	<i>i</i> -Pr	NHCyhex	>20	nd	nd	0.8
34	Cbz	<i>N</i> -guan	<i>s</i> -Bu(<i>S</i>)	NHCyhex	>20	nd	nd	1.3
35	Cbz	<i>N</i> -guan	Bzl	NHCyhex	>20	nd	nd	1.6
36	Cbz	<i>N</i> -guan	CH ₂ Cyhex	NHCyhex	>20	nd	nd	2.1

^aIC₅₀ data represents means ± SEMs for three independent fluorogenic substrate (wtKAHRP) cleavage experiments. *K_m* of substrate was determined for each enzyme batch. A nine-point dilution series of each compound was incubated (37 °C) with *P. falciparum* (Pf) PMVHA isolated from parasites. ^bData represents means ± SEMs for three independent fluorogenic substrate cleavage experiments. An 11-point dilution series of each compound was incubated (25 °C) with cathepsin D. ^cData represents means for two independent TRF substrate cleavage experiments. An 11-point dilution series of each compound was incubated (25 °C) with BACE-1. guan = guanidine; Cyhex = cyclohexyl. ^dCalculated using ChemAxon software.⁴⁵

inhibition values, and in turn, selectivity differences, between PfPMV and PvPMV. To assess whether the compounds were active against human aspartic proteases, they were evaluated for inhibition of β -secretase-1 (BACE-1) and cathepsin D. These aspartic proteases were chosen on the basis that BACE-1 is the human aspartic protease with the closest, albeit distant,

homology to PfPMV (Supporting Information, Figure S5),¹⁴ while cathepsin D shares low sequence similarity with PfPMV (Supporting Information, Figure S6) but is closely related to BACE-1 and is used as a benchmark off-target for BACE-1 drug discovery programs.^{26,27} Accordingly, a BACE-1 time-resolved fluorescence (TRF) assay,²⁸ and a cathepsin D fluorogenic

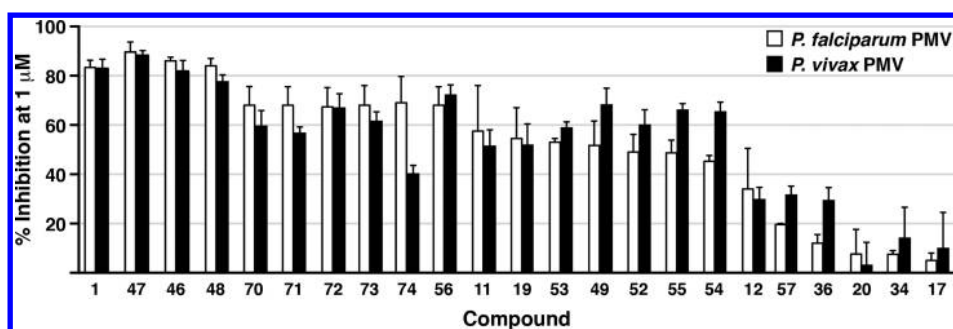


Figure 4. Inhibition of plasmepsin V from *P. falciparum* and *P. vivax*. % Inhibition of PfPMV and PvPMV by the TS mimetics. Percent inhibition of PfPMV and PvPMV were determined by addition of 1 μ M compound into the fluorogenic PEXEL cleavage assay. Results shown are a minimum of three independent biological replicates using either *P. falciparum* (white bar) or *P. vivax* (black bar) PMV. Error bars indicate SEM.

substrate cleavage assay²⁹ was used to assess activity of the compounds.

Structure–Activity Relationship. To investigate the binding selectivity of each region within the mimetics for the corresponding binding pocket in PMV (see Figure 1), the P_3 , P_2 , P_1 , and P_1' moieties of the TS mimetic were sequentially altered and PMV inhibition assessed. The functionality chosen to probe each binding pocket was strongly influenced by the high polar physical characteristics of the TS peptide mimetics, i.e., a hydrophobic functionality was chosen in preference to a hydrophilic group to increase the overall hydrophobicity of the molecule, with a view to improve membrane permeability.

As a starting point, a peptidomimetic was designed based on the common PEXEL motif, RxLxQ. The progenitor peptidomimetic possesses a statine (Sta) in place of the P_1 Leu to mimic the TS tetrahedral intermediate, as well as Ala at P_2 and Arg at P_3 . The carboxy side of the scissile site (i.e., xQ) is somewhat displaced by the additional carbon in Sta, therefore, Gln and Ala were both positioned in the P_1' in two separate molecules, 74 and 11, respectively (Table 1). For simplification at this early stage, the *N*-terminus of both 74 and 11 was capped with *N*-acetamide and the C-terminus with NH_2 amide. The two compounds exhibited IC_{50} values of 556 and 613 nM, respectively, against PfPMV in vitro (Table 1). These results represented an excellent starting point and suggested that the P_1' position was not especially important for activity, as both compounds were approximately equally potent. To test this hypothesis further, the C-terminal group was exchanged for a truncated version of Gln, *N*-propyl amide 12, and also a limited number of hydrophobic functionalities, such as a cyclohexyl substituent (13). The analogues 12 and 13 exhibited slightly less potency (865 and 967 nM, respectively) compared to the Gln 74 and Ala 11 P_1' analogues, and although only a limited number of functionalities were explored at this position, these results demonstrated that the P_1' region is not critical for inhibiting PMV. Additionally, replacing the P_1' residue with a cyclohexyl group (13) increased the overall lipophilicity of the molecule and aided the synthetic tractability of future analogues. Assessment of 13 against PvPMV indicated that inhibitory IC_{50} values were similar to those seen against PfPMV, giving an early indication that both PMV orthologues could be targeted with the same inhibitor. Notably, none of the analogues 11–13 had any observable off-target effects against cathepsin D or BACE-1 ($IC_{50} > 100 \mu M$), suggesting that selectively targeting PMV over human aspartyl proteases was achievable.

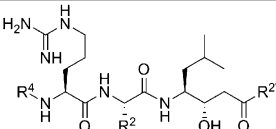
To further aid in the synthesis of future analogues, and again reduce the overall polarity of the molecule(s), it was proposed

to replace the P_4 acetamide group with a Cbz group (19). The *N*-Cbz protective group is orthogonally compatible with the *N,N*-bis Boc functionality used to protect the guanidine located on the P_3 Arg (Schemes 1–6). Additionally, the *N*-Cbz group enhanced the overall lipophilicity of the molecule. Evaluation of the *N*-Cbz analogue 19 demonstrated that it had comparable potency to the *N*-acetamide analogue 13, did not possess off-target protease activity (Table 1), and was therefore a suitable replacement for the P_4 *N*-acetamide functionality. The homology model of PfPMV supported this result, showing that the *N*-Cbz could be accommodated at the P_4 position.

The PEXEL P_3 Arg possesses a guanidine side chain and its substitution with Lys at this position abrogates PEXEL processing and export to the erythrocyte.⁵ Additionally, substitution of Arg with Lys in 1, leading to WEHI-024, blocks inhibition of PfPMV and PvPMV.¹¹ The sensitivity to replacement of the Arg by Lys demonstrates the critical nature of Arg at P_3 . In the homology model of PfPMV, the side chain carboxylates of Glu179 and Glu213 in the S_3 pocket of PMV form salt bridges with the P_3 guanidine of Arg (Figure 3). To further explore the importance of the guanidine side chain at P_3 of the PEXEL, a small set of analogues were synthesized to probe this region. In this set of analogues, the P_3 Arg was replaced by the basic residues ornithine (Orn) (17), Lys (18), and homo Arg (20). The hydrophobic residue homo Phe (75) was also inserted in place of the P_3 Arg; this analogue was generated to investigate whether a bulky hydrophobic residue could be accepted in the S_3 pocket, an approach that has been successful in overcoming the requirement of a guanidine functionality in programs designing inhibitors that target thrombin,³⁰ however, it was not accepted (Table 1). Evaluation of the P_3 analogues 17, 18, 20, and 75 revealed that all of these analogues possessed IC_{50} values $> 20 \mu M$ against PfPMV (Table 1). Similar inhibitory activities were obtained against PvPMV with 17 and 20 (Figure 4), demonstrating the binding requirements of PMV from both *Plasmodium* spp. are similar with respect to the S_3 pocket. Of note, none of the analogues possessed any off-target activity against BACE-1 or cathepsin D, except the homo Phe analogue, 75, which exhibited potent activity against cathepsin D (43 nM) (Table 1). Thus, the functional group at P_3 can be used as a “switch” to tune selectivity toward PMV and away from cathepsin D.

Previous studies have demonstrated that the P_1 Leu is important for PEXEL cleavage in *P. falciparum* and for optimal PMV activity in vitro and in cultured *P. falciparum*.^{5,11} To further examine this, analogues were synthesized that replaced the isobutyl side chain of Sta (19), mimicking Leu, for either an isopropyl (Val) 33, a *sec*-isobutyl (Ile) 34, a benzyl (Phe) 35, or

Table 2. Protease Activity of TS Mimetics, Probing the P₄, P₂, and P₁' / P₂' Moieties

Cmpd				Protease inhibition			cLogP ^e
	R ⁴	R ²	R ^{2'}	PfPMV (±SEM) ^a	cathepsin D (±SEM) ^b	BACE-1 ^c	
19	Cbz	Me	NHCyhex	0.614 (0.143)	>100	>100	1.2
46	Cbz	<i>i</i> -Pr	NHCyhex	0.029 (0.006)	0.713 (0.207)	>100	2.1
47	Cbz	<i>s</i> -Bu(<i>S</i>)	NHCyhex	0.026 (0.007)	0.447 (0.085)	>100	2.5
48	Cbz	<i>i</i> -Bu	NHCyhex	0.077 (0.022)	5.1 (1.8)	>100	2.5
49	Cbz	Bzl	NHCyhex	0.230 (0.050)	4.8 (1.2)	>100	2.8
52	Cbz	Me	NHBzl	0.530 (0.267)	>100	>100	1.1
53	Cbz	Me	NH(CH ₂) ₂ Ph	0.622 (0.355)	29 (14)	>100	1.4
54	Cbz	Me	NH-2-indane	0.772 (0.281)	>100	>100	1.5
55	Cbz	Mc	<i>rac</i> -NHCH(CH ₃)Ph ^d	0.569 (0.239)	>100	>100	1.5
56	Cbz	Me	NH(CH ₂) ₂ Ph(4'-Cl)	0.348 (0.103)	>100	>100	2.0
57	Cbz	Me	NCH ₃ (CH ₂) ₂ Ph(4'-Cl)	2.01 (1.41)	>100	>100	2.2
70	Bz	Mc	NH(CH ₂) ₂ Ph	0.774 (0.699)	>100	>100	0.9
71	BzlOCH ₂ CO	Me	NH(CH ₂) ₂ Ph	0.550 (0.325)	>100	>100	0.6
72	PhSO ₂	Me	NH(CH ₂) ₂ Ph	0.378 (0.269)	>100	>100	0.6
73	PhCH ₂ SO ₂	Me	NH(CH ₂) ₂ Ph	0.625 (0.051)	>100	>100	0.4
1	PhCH ₂ SO ₂	<i>i</i> -Pr	NH(CH ₂) ₂ Ph	0.019 (0.003)	32 (11)	>100	1.3

^aIC₅₀ data represents means ± SEMs for three independent fluorogenic substrate (wtKAHRP) cleavage experiments. A nine-point dilution series of each compound was incubated (37 °C) with *P. falciparum* (Pf) PMVHA isolated from parasites. ^bData represents means ± SEMs for three independent fluorogenic substrate cleavage experiments. An 11-point dilution series of each compound was incubated (25 °C) with cathepsin D. ^cData represents means for two independent TRF substrate cleavage experiments. An 11-point dilution series of each compound was incubated (25 °C) with BACE-1. ^d*rac* = racemic. Cyhex = cyclohexyl. ^eCalculated using ChemAxon software.⁴⁵

a methylcyclohexyl (cyclohexyl Ala) **36** (Table 1). Evaluation of inhibition against PfPMV and PvPMV revealed that none of the analogues **33–36** exhibited activity (IC₅₀ >20 μM or <15% at 1 μM); only the cyclohexylalanine variant **36** displayed weak inhibition (35% at 1 μM) of PvPMV (Figure 4). In the homology model, the PEXEL Leu packs tightly against the hydrophobic residues that line the S₁ site (Figure 3); residues other than Leu would likely pack less well in this pocket. This provides additional evidence that PfPMV and PvPMV both have a strong preference for Leu in the P₁ position.

The P₂ position is primarily denoted as an arbitrary residue (x) in the PEXEL sequence (R_xLxQ/E/D), however, in the PEXEL sequence alignments described by Marti et al.,³ Asn, Ile, Ser, and Leu are common. Our homology model illustrates that the side chain of the P₂ residue makes no substantial interaction with PfPMV. Thus far in this study, Ala had been utilized as the sole P₂ residue. To investigate the residues that could be tolerated in the P₂ region, a select set of analogues were synthesized. Again, hydrophobic residues were chosen in order to reduce the hydrophilic nature of the molecule. In this set of analogues, the P₂ Ala was substituted with Leu, Ile, Val, and Phe to produce the analogues **46**, **47**, **48**, and **49**, respectively (Table 2). The analogues **46–49** were evaluated for inhibitory activity against PfPMV and exhibited a marked improvement in

potency; those with Val or Ile at P₂ (**46** or **47**, respectively) exhibited an approximately 20-fold increase in potency (IC₅₀ of 29 and 26 nM, respectively) compared with the progenitor P₂ Ala surrogate, **19**. The P₂ Leu analogue **48** (IC₅₀ = 77 nM) was marginally weaker than the Val or Ile orthologues (**46** and **47**, respectively), and the P₂ Phe analogue, **49**, was weaker again (IC₅₀ = 230 nM) (Table 2). In the homology model, Cys178 lies in close proximity to the P₂ residue; the hydrophobic nature of Cys may explain the improved affinity of hydrophobic groups at this position in the inhibitors. Inhibition of PvPMV by **46–49** correlated well with the results obtained against PfPMV (Figure 4). Although no off-target inhibition on BACE-1 was observed, significant inhibition of cathepsin D was observed with analogues **46** (IC₅₀ = 713 nM) and **47** (IC₅₀ = 447 nM) and to a lesser degree **48** (IC₅₀ = 5.1 μM) and **49** (IC₅₀ = 4.8 μM). The MEROPS online database³¹ includes a number of substrates that are processed by cathepsin D and which harbor hydrophobic amino acids such as Val or Leu at the P₂ position. This is reflected in the activity of the Val or Ile orthologues (**46** and **47**) against cathepsin D.

The next step was to examine the C-terminal P₁' / P₂' region of the mimetics, and for this parallel chemistry was employed to generate a large number of analogues. The inhibitory effect against PMV was determined at 1 μM before determining the

IC₅₀ values of selected analogues. First, an array of amides were generated in parallel (parallel set 1; Supporting Information, Scheme S1 and Table S1) and then evaluated for inhibitory activity at 1 μ M. The inhibitory activity of **D2** (51% at 1 μ M) compared well to the previously synthesized C-terminal cyclohexyl amide **19** (54% at 1 μ M). However, disubstitution on the C-terminal amide nitrogen (**A3**, **B3**, **C3**, **D3**, **A6**, **B6**, and **C6**; <32% inhibition at 1 μ M) was detrimental to activity, which can be attributed to the loss of the C-terminal N–H interaction with the backbone carbonyl oxygen of Gly120. Analogues with substitution on the *N*- α -carbon (**A2**, **B2**, **C2**, **A5**, **C5**, and **D5**; 51–66% inhibition at 1 μ M) all possessed similar activity to the progenitor cyclohexyl amide analogue **D2** (**19**). Smaller *N*-amide substituents such as *n*-propyl **A4**, isopropyl **B4**, and isobutyl **C4** also possessed similar potency (42–56% inhibition at 1 μ M) to the cyclohexyl amide **19**. The *N*-benzyl **B1**, *N*-indane **C5**, *N*-ethylphenyl **C1**, and *N*-propylphenyl **D1** amides were found to be more potent than the cyclohexyl amide **D2** (**19**), presumably due to the additional lipophilicity, in comparison to the analogues **A4**–**C4**.

To determine IC₅₀ values, six of the above amides were selected for resynthesis (Scheme 5) and nine-point titrations against PfPMV (Table 2). This confirmed the results obtained with the parallel set: *N*-disubstitution on the amide (**57**, IC₅₀ of 2.0 μ M) was poorly tolerated, and *N*-ethylphenyl analogues, **53** and **56** (IC₅₀ of 622 and 348 nM), were comparatively as potent as the *N*-benzyl amides, **55** and **52** (IC₅₀ of 569 and 530 nM). The P₁/P₂' analogues had slightly greater potency for PvPMV than PfPMV, revealing that small differences exist between the two active sites. Only the *N*-ethylphenyl derivative, **53**, displayed off-target activity, having weak activity against cathepsin D (IC₅₀ = 29 μ M). Intriguingly, the *N*-ethyl 4'-chlorophenyl analogue, **56**, exhibited no activity against cathepsin D (IC₅₀ >100 μ M). In summary, alterations to the C-terminal P₁'/P₂' region of the mimetics resulted in only subtle differences in inhibitory profile, the exception being the disubstitution of the C-terminal nitrogen. The lack of sensitivity to substitution in this region provides evidence that the x/Q/E/D portion of the PEXEL sequence motif is not important for inhibition of PMV, consistent with the observed functional specificity of PEXEL cleavage⁹ and PfPMV activity.¹³ The *N*-ethylphenyl amide was selected for integration into the P₁'/P₂' position to undertake future chemistries in this study.

We next explored modifications to the *N*-terminal P₄ region in an attempt to further enhance potency and again employed a parallel chemistry approach. To undertake the parallel chemistry, the P₃ guanidine functionality was Boc protected and the P₁ Sta hydroxyl functionality was protected with TBDMS, allowing a parallel series of acylation reactions to be performed on the exposed *N*-terminus (parallel set 2; Supporting Information, Scheme S2). A set of hydrophobic acid chlorides, sulfonyl chlorides, and isocyanates were used to perform acylation of the *N*-terminus in parallel (parallel set 2; Supporting Information, Table S2). Both the Boc and TBDMS protection was subsequently removed in one step using TFA. Compounds were then evaluated for inhibitory activity against PfPMV (parallel set 2; Supporting Information, Table S3). Inhibition by **K3** (71% at 1 μ M) compared well to the previously synthesized C-terminal *N*-ethylphenyl amide **53** (54% at 1 μ M) (Table 2). However, a urea in the P₄ position was detrimental to activity (**I5**, **J5**, and **L5**; <41% inhibition at 1 μ M). The substituted alkyl acetamides (**I1**, **J1**, and **K1**) and the carbamates (**I3** and **J3**) did not improve activity (<49%

inhibition at 1 μ M), and the substituted aryl acetamides (**I2**, **J2**, **K2**, and **L2**) possessed comparable activity (59–81% inhibition at 1 μ M) to the progenitor Cbz analogue **K3**. However, the sulfonamides **J4**, **K4**, **L4**, and **L3** resulted in a slight improvement in potency (78–89% inhibition at 1 μ M) (parallel set 2; Supporting Information, Table S3).

To determine IC₅₀ values, selected compounds were chosen for resynthesis (Scheme 6) and eight-point titrations against PfPMV (Table 2). Retesting confirmed that the phenylsulfonyl amide **72** (IC₅₀ = 378 nM) was more potent than both the benzylsulfonyl **73** (IC₅₀ = 625 nM) and benzyloxycetamide **71** (IC₅₀ = 550 nM) analogues. The benzamide derivative **70** (IC₅₀ = 774 nM) possessed the weakest activity of this set. This select set of compounds **70**–**73** displayed negligible difference in selectivity between PfPMV and PvPMV (Figure 4). We also observed that a sulfonamide is more favorable than an amide (**72** compared to **70**) for binding affinity, suggesting either that the sulfonyl performs an additional interaction that is not possible with an amide or that the sulfonamide group projects the adjoining substituent in a more preferable orientation for binding to PMV than the corresponding amide. In summary, the P₄ region immediately surrounding the *N*-terminus of the P₃ residue plays only a small role in modulating activity against PMV.

Finally, we synthesized compound **1** that incorporated the sum of optimal modifications determined above. This comprised of the phenylsulfonyl amide at P₄, Arg at P₃, Val at P₂, and Leu(Sta) at P₁, followed by *N*-ethylphenyl amide at P₁'/P₂' (Table 2). Compound **1**¹¹ potentially inhibited PfPMV and PvPMV (IC₅₀ = 19 nM and 24 nM, respectively) and showed no off-target activity against BACE-1 and little activity against cathepsin D (IC₅₀ = 32 μ M). The off-target selectivity window of **1** between PfPMV and cathepsin D (1300-fold) is a vast improvement compared to compound **46** (20-fold). The selectivity of **1** demonstrates that, while modification of the *N*-terminal P₄ and C-terminal P₁'/P₂' regions only slightly influences affinity for PMV, it impacts greatly on selectivity for cathepsin D. As such, it should be possible to develop highly selective and potent analogues that uniquely target PMV.

Inhibition of PEXEL Cleavage by PMV in Parasites. A selection of eight TS mimetics of varying activity (IC₅₀ ranging from 0.019 to >20 μ M against PMV in vitro) was assessed for their ability to inhibit PMV activity in parasites. To assess this, transgenic *P. falciparum* expressing the exported PEXEL protein *P. falciparum* erythrocyte membrane protein 3 (PfEMP3) fused to green fluorescent protein (GFP)¹³ were treated with compounds for 5 h and the processed and unprocessed species were visualized by immunoblot with anti-GFP antibodies.^{11,13} Compounds **72**, **46**, **47**, and **1** inhibited PEXEL processing to varying degrees; uncleaved PfEMP3-GFP (black arrow) could be observed and was the same size as uncleaved PEXEL R > A mutant PfEMP3-GFP^{11,13} (Figure 5). PEXEL-cleaved (blue arrow) and “GFP only” (degraded reporter in the food vacuole; ~26 kDa) species of PfEMP3-GFP were also visible (Figure 5). The degree of activity against PMV in parasites correlated well with the observed activity against PMV in vitro (refer to Table 3), with compound **17** among the least and **1** the most active (Figure 5, Supporting Information, Figure S1). For **17**, this correlated with the lack of activity against PMV in vitro (IC₅₀ >20 μ M), which can be attributed to an ornithine mimetic in place of arginine at P₃ of the compound.^{5,11} However, compounds **19**, **71**, **48**, and **46** had no significant effect on PEXEL processing of PfEMP3-GFP in parasites despite having

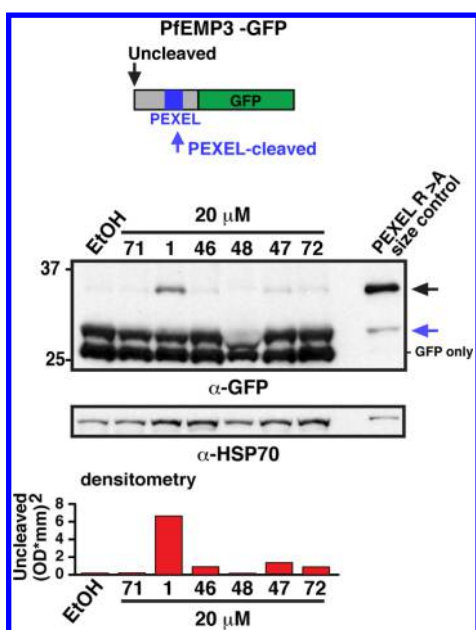


Figure 5. Activity of selected transition state mimetics against PMV in cultured parasites. *P. falciparum* trophozoites expressing PfEMP3-GFP in infected erythrocytes were treated with 20 μM of compound 71, 1, 46, 48, 47, 72, or vehicle control (EtOH) and processing of the PEXEL in PfEMP3 was assessed by immunoblotting with anti-GFP antibodies. A schematic of the GFP protein and its cleavage positions is shown at the top. Uncleaved (black arrow), PEXEL-cleaved (blue arrow), and “GFP only” (a degraded remnant of the GFP reporter in the food vacuole) species of PfEMP3-GFP are indicated next to the immunoblot. PEXEL R > A mutant PfEMP3-GFP was included as a size control, and the blot was probed with parasite anti-HSP70 as a loading control. Densitometry of the uncleaved band in each lane is shown beneath the blot. PMV inhibition can be seen for compounds 1, 46, 47, and 72.

IC₅₀ values <0.6 μM against PfPMV in vitro (Table 3, Figure 5, Supporting Information, Figure S1). The weak cellular activity of these compounds suggests that they possess suboptimal properties for accessing PMV in the parasite ER, which may include poor membrane permeability, likely influenced by their peptidic and polar nature. Our attempts to overcome the polar guanidine side chain of Arg at P₃ in our compounds consistently abolished inhibitory activity, illustrating the exquisite selectivity of PMV and a key challenge to overcome if inhibitors are to become orally bioavailable.

Viability of Treated Parasites and Human Cell Lines.

The effect of the TS mimetics on parasite viability was assessed by treating early ring-stage *P. falciparum* 3D7 parasites with compounds, or vehicle controls, and measuring parasitemia 72 h later by flow cytometry. Chloroquine was included in these experiments as a positive control. Parasite survival is summarized in Table 3 and Supporting Information Figure S4 and correlated well with the degree of PfPMV inhibition in vitro, with the two most potent inhibitors, 1 and 47 (IC₅₀ 19 and 26 nM, respectively), having the greatest effect on parasite viability (EC₅₀ 2.5 and 6.8 μM, respectively). 47 was less active against parasites than 1 and had a weaker effect on PfEMP3 PEXEL cleavage in parasites (Figure 5), suggesting 47 has less access to PMV in the ER than 1.

For some compounds, parasite death could not solely be attributed to PMV inhibition. For example, compounds 48, 71, and 19, which displayed inhibitory activity in vitro (IC₅₀ 0.077,

Table 3. Cellular Activity of TS Mimetics Compared to *P. falciparum* PMV Inhibition

compd	PfPMV IC ₅₀ (μM) ^a	<i>P. falciparum</i> viability EC ₅₀ (μM) ^b	densitometry of PfEMP3 PEXEL cleavage inhibition ^c	HepG2 EC ₅₀ (μM) ^d	cLogP ^e
17	>20	>50	0.18 (0.08)	>50	2.3
19	0.614 (0.143)	34.6 (5.9)	0.20 (0.10)	>50	1.2
71	0.550 (0.325)	23.0 (6.7)	0.16 (0.01)	>50	0.6
72	0.378 (0.269)	16.3 (1.1)	0.31 (0.04)	nd	0.6
48	0.077 (0.022)	8.9 (1.3)	0.26 (0.14)	>50	2.5
46	0.029 (0.006)	9.8 (1.5)	0.24 (0.05)	>50	2.1
47	0.026 (0.007)	6.8 (0.3)	0.53 (0.13)	>50	2.5
1	0.019 (0.003)	2.5 (0.5)	2.76 (0.58)	>50	1.3
CQ ^f	nd	0.003 (0.002–0.004)	nd	nd	nd

^aIC₅₀ data represents mean (±SEM) of three independent fluorogenic substrate (wtKAHRP) cleavage experiments. A nine-point dilution series of each compound was incubated with *P. falciparum* (Pf) PMVHA isolated from parasites. ^bEC₅₀ data represents mean ± SEMs for three independent experiments measuring *P. falciparum* 3D7 parasitemia by flow cytometry following exposure to compounds in nine-point dilution series for 72 h. Parasite survival was measured relative to vehicle-treated controls. ^cData is the mean (±SEM) of three experiments measuring inhibition of PfEMP3-GFP PEXEL processing in *P. falciparum*-infected erythrocytes following treatment with 20 μM compound for 5 h. PEXEL cleavage was evaluated by immunoblot with anti-GFP antibodies and densitometry of the uncleaved bands (optical density per mm²) was performed. ^dIC₅₀ data represents mean of three independent toxicity experiments. An 11-point dilution series of each compound was incubated for 48 h. Cell Titer-Glo was used to quantify cell death. ^eCalculated using ChemAxon software.⁴⁵ ^fCQ, chloroquine.

0.550, and 0.614 μM, respectively) but did not inhibit PEXEL processing in parasites, were toxic to parasites, with EC₅₀ values of 8.9, 23, and 34.6 μM, respectively (Table 3). Thus, some mimetics hit off-targets and these may include other parasite aspartyl proteases (e.g., plasmepsins). There are 10 plasmepsin enzymes encoded in the *P. falciparum* genome, however, not all are expressed in the blood stage and some are known to be nonessential. For example, plasmepsins I–IV and VII are dispensable for parasite development,^{21,32} and off target inhibition of these aspartyl proteases is unlikely to account for parasite death in our study. A possible off-target is plasmepsin IX, which is expressed in the blood stage; however, it has been shown previously not to cleave the PEXEL motif¹³ and its function and essentiality is presently unknown. Other aspartyl protease inhibitors that kill malaria parasites have been described;³³ however, their essential parasite target(s) are also presently unknown.

The TS mimetics were not broadly cytotoxic to HepG2 cells (Table 3) and had little effect against the human aspartyl proteases BACE-1 and cathepsin D (Tables 1 and 2), demonstrating that PMV can be selectively inhibited over

human aspartyl proteases and is a valid target for novel, future antimalarial intervention.

CONCLUSIONS

The results presented in this study demonstrate the narrow selectivity profile of both PfPMV and PvPMV. Utilizing TS mimetics as probes, we have shown that the sites within PMV that bind the P₁ and P₃ groups confer strict restrictions on the functionality that can be accommodated at these positions. This was highlighted when the P₁ Leu was exchanged for a P₁ Ile mimetic, or the P₃ Arg was exchanged for a P₃ Lys or ornithine mimetic, and all PMV inhibitory activity was lost. This narrow selectivity window is attributed to the exclusive preference of PMV for the first three residues of the PEXEL sequence, RxL. However, this study has also highlighted the P₂ residue, although not critical for binding PMV, as highly important for modulating affinity for it. An example was the 20-fold improvement in potency achieved by a small change from a methyl (P₂ alanine) **19** to an isopropyl (P₂ valine) **46**. Indeed, the presence of Val at this position of the PEXEL is common in *P. falciparum* proteins.⁶ Beyond the P₁–P₃ region, the P₄ and P₁'/P₂' regions of the mimetics could be significantly changed without considerably altering the binding affinity for PMV (Figure 6). PMV from *P. falciparum* or *P. vivax* demonstrate very similar substrate specificities and compound selectivities despite sharing only 54.7% sequence identity (82.2% similarity).¹¹

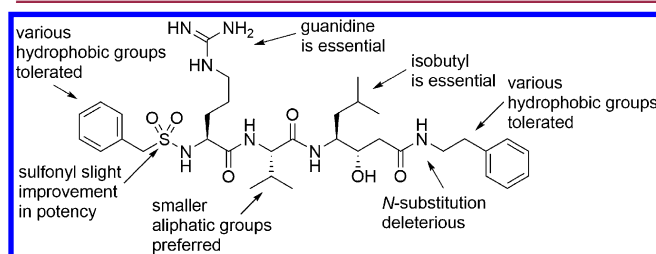


Figure 6. Summary of the key structure–activity relationships, using **1**.

The unique selectivity profile of PMV was also made evident with the off-target protease selectivity data presented in this study. These results demonstrated that the off-target BACE-1 and cathepsin D activity could be regulated through definitive changes to the TS mimetic structure. This was highlighted when the P₃ arginine of **19** was replaced with homo phenylalanine in analogue **75**; the inhibitory activity for PMV was entirely lost but resulted in a 2000-fold enhancement in potency for cathepsin D. This data provides preliminary evidence that PMV can be selectively targeted in future medicinal chemistry programs.

The mimetics in this study were refined by a rational approach and produced potent inhibitors of PMV, several of which are in the low nanomolar range. The most potent compounds exhibited a moderate effect in a parasite viability assay, and there was good correlation between PMV inhibition and parasite viability. Functionally, it was demonstrated that a small molecule inhibitor of PMV was able to reduce PEXEL processing efficiency in *P. falciparum*-infected erythrocytes. Future medicinal chemistry efforts will be primarily focused on improving physicochemical properties of PMV inhibitors, with the view to generate compounds with enhanced permeability that better access the ER and have a greater functional effect in parasites as a direct result of PMV inhibition. The mimetic

probes described have been utilized to generate data that further validates the position of PMV as an essential enzyme for parasite survival in human erythrocytes and as a target for small molecule intervention of malaria.

EXPERIMENTAL SECTION

Molecular Modeling. Comparative modeling was performed using the MODELER program³⁴ employing the X-ray crystal structures of plasmepsin II from *P. falciparum* (2BJU),³⁵ plasmepsin from *P. vivax* (1QS8),³⁶ human BACE-1 (2VIE),³⁷ and the secreted aspartic protease (3PVK)³⁸ as templates. The resulting model was subjected to molecular dynamics (MD) simulation using the GROMACS (v4.5.5) program³⁹ employing the OPLS-aa force field.⁴⁰ The system was solvated in a box of water (TIP4P). Ionizable residues were fixed in their charged state, and the system neutralized and the ionic concentration adjusted to 0.1 M by including Na⁺ and Cl[−] ions. Protein and ligand with water and ions were coupled separately to a thermal bath at 300 K using velocity rescaling⁴¹ applied with a coupling time of 0.1 ps, and the pressure was coupled to an isotropic barostat using a time constant of 1 ps and compressibility of $4.5 \times 10^{-5} \text{ bar}^{-1}$. All simulations were performed with a single nonbonded cutoff of 10 Å and applying a neighbor-list update frequency of 10 steps (20 fs). The particle-mesh Ewald method⁴² was used to account for long-range electrostatics, applying a grid width of 1.2 Å and a fourth-order spline interpolation. Bond lengths were constrained using the LINCS algorithm.⁴³ The system was initially minimized prior to MD simulation and followed by two rounds of positional restrained MD, initially with all protein non-hydrogen atoms restrained to their original positions for 0.1 ns, then with restraints on backbone atoms only in regions of α helix or β sheet for 1.0 ns. This was followed by 10 ns of unrestrained MD.

Plasmepsin V-Agarose and Fluorogenic PEXEL Cleavage Assays. PMV-agarose and PEXEL cleavage assays were performed as described previously.^{5,11,13} Briefly, PMV-agarose was prepared by purification of HA-tagged *P. falciparum* or *P. vivax* PMV from transgenic *P. falciparum* parasite lysates using affinity chromatography with goat anti-HA agarose (Abcam). The digest was obtained as described above and was used at a final assay concentration of 0.15 $\mu\text{L}/20 \mu\text{L}$. The KAHRP PEXEL peptide substrate DABCYL-RNKRTLQKQ-E-EDANS was obtained commercially and used at a final assay concentration at the enzyme K_m (the K_m of substrate was calculated for each PMV-agarose batch). To reduce variation between assays and batches of PMV-agarose, the K_m of PMV cleavage of the KAHRP peptide was calculated and such conditions used for each batch of PMV-agarose. The end-point for all assays was set within the linear range of activity (approximately 2 h). Tween-20 was used at 0.005% final assay concentration. Final assay buffer concentration was as follows: 25 mM Tris HCl, 25 mM MOPS (pH 6.4). Final assay volume was 20 μL . A nine-point $1/2$ serial dilution of compounds was generated using DMSO as a vehicle (final assay concentration of 1%). Assay reaction was incubated for 120 min at 37 °C and read using a fluorescence plate reader (Ex 340 nm, Em 495 nm). IC₅₀ values were determined using a nonlinear regression four-parameter fit analysis, where two of the parameters were constrained to 0 and 100%.

BACE-1 Time-Resolved Fluorescence Assay. A similar procedure was followed according to Porcari et al.²⁸ BACE-1 was obtained commercially and used at a final assay concentration of 312.5 fg/1 μL . The substrate Ac-Cys-(Eu chelate)-Glu-Val-Asn-Leu*-Asp-Ala-Glu-Phe-Lys-QSY7-NH₂ was obtained commercially and used at a final assay concentration 19 μM . NaOAc was used as a buffer (pH 4) at a 50 mM final assay concentration. Tween-20 was used at 0.005% final assay concentration. An 11-point $1/3$ serial dilution of compounds was performed using DMSO as a vehicle (final assay concentration of 1%). Final assay volume was 30 μL . Assay reaction was incubated for 90 min at 25 °C and read using a fluorescence plate reader (Ex 340 nm, Em 615 nm, 400 μs delay). IC₅₀ values were determined using a nonlinear regression four-parameter fit analysis, where two of the parameters were constrained to 0 and 100%. Compounds from the literature were used as controls; the 2-amino-3,4-dihydroquinazoline

compound **3a** from Baxter et al.²⁶ reported an IC_{50} of 11 nM (K_i), obtained 5 nM (SEM \pm 0.0 nM); the aminohydantoin compound **2** from Malamas et al.²⁷ reported an IC_{50} of 3.4 μ M, obtained 4.1 μ M (SEM \pm 0.6 μ M).

Cathepsin D Fluorogenic Substrate Assay. A similar procedure was followed according to Yasuda et al.²⁹ Cathepsin D was obtained commercially and used at a final assay concentration of 40 fg/1 μ L. The substrate MOCAC-Gly-Lys-Pro-Ile-Leu-Phe^{*}-Phe-Arg-Lys-(DNP)-Asp-Arg-NH₂ was obtained commercially and used at a final assay concentration of 19 μ M. NaOAc was used as a buffer (pH 4) at a 100 mM final assay concentration. An 11-point $1/3$ serial dilution of compounds was performed using DMSO as a vehicle (final assay concentration of 1%). Final assay volume was 30 μ L. Assay reaction was incubated for 60 min at 25 °C and read using a fluorescence plate reader (Ex 340 nm, Em 405 nm). IC_{50} values were determined using a nonlinear regression four-parameter fit analysis, where two of the parameters were constrained to 0 and 100%. Compounds from the literature were used as controls: the 2-amino-3,4-dihydroquinazoline compound **3a** from Baxter et al.²⁶ reported an IC_{50} of 110 nM, obtained 46 nM (\pm SEM 15 nM); the aminohydantoin compound **2** from Malamas et al.²⁷ reported an IC_{50} of 100 μ M, obtained 11.8 μ M.

HepG2 Viability Assay. HepG2 cells were cultured in Dulbecco's Modified Eagles Medium (DME) supplemented with 10% heat-inactivated fetal calf serum (FCS) in a humidified incubator at 37 °C and 5% CO₂. Eleven-point compound titration assays were performed by treating cells (1×10^4) for 48 h in 96-well plates. Cytotoxicity was determined using CellTiter Glo (Promega) and calculated as a percentage of DMSO control. Compound TCMD-136775 from literature⁴⁴ was used as a control compound and reported a 17% inhibition at 10 μ M, obtained an IC_{50} of 19 μ M (\pm SEM 2.3 μ M).

***P. falciparum* Culture, Parasite PEXEL Cleavage Assays, Immunoblots, and Densitometry.** *P. falciparum* 3D7 were cultured in human O⁺ erythrocytes at 4% hematocrit in RPMI 1640 medium supplemented with 25 mM HEPES, pH 7.4, 0.2% sodium bicarbonate, and 0.5% Albumax II (Invitrogen) in culture gas (5% CO₂, 5% O₂, 90% N) at 37 °C. Transgenic *P. falciparum* expressing PfEMP3-GFP from the CRT promoter were generated previously¹³ and treated with compounds as described previously.¹¹ Briefly, 30–34 h old trophozoites were purified from uninfected erythrocytes by passing through a Vario Macs magnet column (Miltenyi Biotech) and treated with inhibitor for 5 h at 37 °C in culture gas. Parasites were treated with 0.1% saponin and pellets solubilized in 4 \times Laemmli sample buffer before protein separation via SDS-PAGE. Proteins were transferred to nitrocellulose using an iBlot (Invitrogen), blocked in 10% skim milk/PBS-T and probed with mouse anti-GFP (Roche; 1:1000), rabbit anti-HSP70 (1:4000), or rabbit anti-Aldolase (1:1000) antibodies followed by horseradish peroxidase-conjugated secondary antibodies (Silenius; 1:2000) and visualized using enhanced chemiluminescence (Amersham). Densitometry of blots exposed within the linear range were scanned at 400 dpi using a GS-800 calibrated densitometer (Bio-Rad) and quantified in Quantity One v4.6.3 software (Bio-Rad).

Parasite Viability Assays. Parasite viability assays were performed as described previously.¹¹ Briefly, early ring-stage *P. falciparum* 3D7 parasites were obtained by sorbitol synchronization and treated in 96-well plates with compounds dissolved in ethanol (not greater than 2% final to limit toxicity) or DMSO (not greater than 0.2% final to limit toxicity) in nine-point titrations for 72 h at 37 °C in culture gas. Parasitemia was then determined by flow cytometry and expressed relative to vehicle-treated controls. Parasitemia was qualitatively assessed by Giemsa smears.

Data Analyses. All data were analyzed using GraphPad Prism 6. IC_{50} and EC_{50} sigmoidal dose–response curves were constrained to 0 and 100% relative to vehicle controls.

General Chemistry Procedures. Analytical thin-layer chromatography was performed on Merck silica gel 60F²⁵⁴ aluminum-backed plates and visualized by fluorescence quenching under UV light or by KMnO₄ staining. Flash chromatography was performed with silica gel 60 (particle size 0.040–0.063 μ m). NMR spectra were recorded on a Bruker Avance DRX 300 with the solvents indicated (¹H NMR at 300 MHz). Chemical shifts are reported in ppm on the δ scale and

referenced to the appropriate solvent peak. MeOD contains H₂O. HRMS were acquired by Jason Dang at the Monash Institute of Pharmaceutical Sciences Spectrometry Facility using an Agilent 1290 infinity 6224 TOF LCMS. Column used was RRHT 2.1 mm \times 50 mm 1.8 μ m C18. Gradient was applied over the 5 min with the flow rate of 0.5 mL/min. For MS: gas temperature was 325 °C; drying gas 11 L/min; nebulizer 45 psig, and the fragmentor 125 V. LCMS were recorded on a Waters ZQ 3100 using a 2996 diode array detector. LCMS conditions used to assess purity of compounds were as follows: column, XBridge TM C18 5 μ m 4.6 mm \times 100 mm; injection volume 10 μ L; gradient, 10–100% B over 10 min (solvent A, water 0.1% formic acid; solvent B, AcCN 0.1% formic acid); flow rate, 1.5 mL/min; detection, 100–600 nm. All final compounds were analyzed using high performance liquid chromatography/ultraviolet/evaporative light scattering detection coupled to mass spectrometry. Unless otherwise noted, all compounds were found to be >95% pure by this method.

The following compounds were purchased commercially and used without further purification: Cbz-Orn(N-Boc)-OH, Cbz-Lys(N-Boc)-OH, Fmoc-Sta(S,S)-OH, Boc-Sta(S,S)-OH, HCl-NH₂-Ala-OEt, HCl-NH₂-Val-OMe, HCl-NH₂-Leu-OMe, HCl-NH₂-Ile-OMe, HCl-NH₂-Phe-OEt, 4-aminobutyric acid amide hydrochloride, Boc-AHPA-OH, Boc-ACHPA-OH, Boc-AHMHpA-OH, and Boc-AHMHxA-OH. Ac-Arg(NH₂)-Ala-Sta-Gln-CONH₂·TFA **74** was synthesized using solid phase methods by John Karas at ModPep, Melbourne, Australia. PhCH₂SO₂-Arg(NH₂)-Val-Sta-NH(CH₂)₂Ph·TFA **1** was synthesized as previously described.¹¹

General Procedure D. HCl-NH₂-Sta-NHCyhex (6). A mixture of Boc-Sta-NHCyhex **80** (650 mg, 1.82 mmol) in a mixture of 4 N HCl in dioxane (4.0 mL) was allowed to sit for 2 h at 20 °C. The reaction mixture was concentrated to dryness in vacuo to obtain a solid. The solid was triturated with Et₂O and filtered off to obtain **6** as a white solid (530 mg, 98%). ¹H NMR (DMSO-*d*₆): δ 8.01 (d, 1H, *J* 8.0 Hz), 7.88 (br s, 3H), 3.89–3.86 (m, 1H), 3.55–3.51 (m, 1H), 3.02 (br s, 1H), 2.52 (m, 1H), 2.29 (m, 1H), 1.71–1.05 (m, 13H), 0.88–0.84 (m, 6H).

NH₂-Sta-NH(CH₂)₂Ph-HCl (7). General procedure D was followed using Boc-Sta-NH(CH₂)₂Ph **115** (950 mg, 2.51 mmol) to obtain **7** as a hygroscopic residue (780 mg, 99%). ¹H NMR (600 MHz, MeOD) δ 7.25–7.11 (m, 5H), 3.98–3.92 (m, 1H), 3.38 (t, *J* = 7.4 Hz, 2H), 3.20–3.14 (m, 1H), 2.76 (t, *J* = 7.4 Hz, 2H), 2.51 (dd, *J* = 14.8, 5.3 Hz, 1H), 2.42 (dd, *J* = 14.8, 6.9 Hz, 1H), 1.74–1.65 (m, 1H), 1.56–1.48 (m, 1H), 1.47–1.40 (m, 1H), 0.92 (d, *J* = 6.5 Hz, 6H). *m/z* = 279 [M + H]⁺.

Ac-Orn(N-Boc)-Ala-OEt (9). A mixture of Cbz-Orn(N-Boc)-Ala-OEt **76** (3.0 g, 6.44 mmol) and Pd/C (0.03 mmol) in EtOAc (100 mL) was allowed to stir for 2 h at 20 °C under a hydrogen atmosphere. The reaction mixture was filtered through a bed of Celite and washed with EtOAc. Acetic anhydride (855 μ L, 8.83 mmol) and Et₃N (898 μ L, 6.44 mmol) was added, and the resulting mixture was then allowed to stir at 20 °C under a nitrogen atmosphere for 2 h. Water (50 mL) was added to the reaction mixture. The layers were then separated. The organic layer was dried (MgSO₄), and the organic layer was concentrated in vacuo to obtain a solid. The solid was triturated with Et₂O and filtered off, washing with Et₂O to obtain **9** as a white solid (2.3 g, 95%). ¹H NMR (CDCl₃): δ 7.03 (br s, 1H), 6.51 (d, 1H, *J* 8.0 Hz), 4.83–4.79 (m, 1H), 4.62 (br s, 1H), 4.54–4.45 (m, 1H), 4.20–4.12 (m, 2H), 3.32–3.27 (m, 1H), 3.11–3.02 (m, 1H), 2.00 (s, 3H), 1.86–1.83 (m, 2H), 1.63–1.55 (m, 2H), 1.42–1.39 (m, 12H), 1.26 (t, 3H, *J* 7.1 Hz). MS, *m/z* = 374 [M + H]⁺.

General Procedure B. Ac-Arg(N,N-diBoc)-Ala-OH (10). A mixture of Ac-Arg(N,N-diBoc)-Ala-OEt **77** (550 mg, 1.07 mmol) and LiOH (51 mg, 2.13 mmol) in a mixture of water (3 mL) and THF (5 mL) was allowed to stir for 2 h at 20 °C. Citric acid solution was added to the reaction mixture. The solution was extracted with EtOAc (2 \times 20 mL). The organic layer was then washed with brine solution (1 \times 20 mL). The organic layer was dried (MgSO₄), and the organic layer was concentrated in vacuo to obtain **10** as a foam (505 mg, 97%). ¹H NMR (CDCl₃): δ 8.52 (br s, 1H), 7.59 (d, 1H, *J* 8.0 Hz), 7.02 (d, 1H, *J* 7.1 Hz), 4.57–4.47 (m, 2H), 3.44–3.31 (m, 2H), 2.06 (s, 3H), 1.93–1.66 (m, 4H), 1.50–1.47 (s, 21H). MS, *m/z* = 490 [M + H]⁺.

General Procedure E. *Ac-Arg(NH₂)-Ala-Sta-Ala-NH₂-TFA (11).* A mixture of *Ac-Arg(N,N-diBoc)-Ala-Sta-Ala-NH₂* **81** (35 mg, 0.05 mmol) in TFA (0.5 mL) and DCM (1 mL) was allowed to stir for 6 h at 20 °C. The reaction mixture was concentrated to dryness in vacuo. The oil was triturated with Et₂O and filtered off, washing with Et₂O to obtain **11** as a white solid (35 mg, 48%). ¹H NMR (MeOD) (rotamers): δ 4.39–4.28 (m, 3H), 4.07–3.97 and 3.65–3.55 (2 × m, 2H), 3.25–3.20 (m, 2H), 2.80–2.70 and 2.41–2.34 (2 × m, 2H), 2.01 (s, 3H), 1.90–1.25 (m, 13H), 1.01–0.92 (m, 6H). HRMS found: (M + H) 515.3293; C₂₂H₄₂N₈O₆ requires (M + H), 515.3306.

Ac-Arg(NH₂)-Ala-Sta-NH(CH₂)₃CONH₂-TFA (12). General procedure E was followed using *Ac-Arg(N,N-diBoc)-Ala-Sta-NH-(CH₂)₃CONH₂* **83** (20 mg, 0.027 mmol) to obtain **12** as a white solid (13 mg, 74%). ¹H NMR (MeOD): δ 4.39–4.26 (m, 2H), 4.02–3.98 (m, 2H), 3.27–3.20 (m, 4H), 2.37–2.24 (m, 4H), 1.86 (s, 3H), 1.85–1.20 (m, 12H), 1.01–0.85 (m, 6H). HRMS found: (M + H) 529.3457; C₂₃H₄₄N₈O₆ requires (M + H), 529.3462.

Ac-Arg(NH₂)-Ala-Sta-NHCyhex-TFA (13). General procedure E was followed using *Ac-Arg(N,N-diBoc)-Ala-Sta-NHCyhex* **84** (25 mg, 34.4 mmol), to obtain **13** as a white solid (10 mg, 45%). ¹H NMR (MeOD): δ 4.38–4.25 (m, 2H), 4.00–3.90 (m, 2H), 3.69–3.60 (m, 1H), 3.23–3.19 (m, 2H), 2.31–2.24 (m, 2H), 2.01 (s, 3H), 1.89–1.20 (m, 20H), 1.00–0.85 (m, 6H). HRMS found: (M + H) 526.3707; C₂₅H₄₇N₇O₅ requires (M + H), 526.3717.

Cbz-Orn(N-Boc)-Ala-OH (15). General procedure B was followed using *Cbz-Orn(N-Boc)-Ala-OEt* **76** (100 mg, 0.22 mmol) to obtain **15** as an oil (90 mg, 98%). ¹H NMR (CDCl₃) (rotamers): δ 7.34 (s, 5H), 7.20 (br s, 0.5H), 6.30 (br s, 0.5H), 6.12 (br s, 0.5H), 5.95 (br s, 1H), 5.11 (s, 2H), 4.98 (br s, 0.5H), 4.56–4.30 (m, 2H), 3.25–3.00 (m, 2H), 1.90–1.35 (m, 16H). MS, *m/z* = 438 [M + H]⁺.

Cbz-Lys(N-Boc)-Ala-OH (16). General procedure B was followed using *Cbz-Lys(N-Boc)-Ala-OEt* **86** (1.0 g, 2.09 mmol) to obtain **16** as an oil (900 mg, 96%). ¹H NMR (CDCl₃): δ 7.35 (s, 5H), 7.00 (d, 1H, *J* 7.6 Hz), 5.88 (br s, 1H), 5.11 (s, 2H), 4.45–4.48 (m, 1H), 4.27–4.24 (m, 1H), 3.10–3.00 (m, 2H), 1.89–1.81 (m, 2H), 1.71–1.64 (m, 2H), 1.46–1.43 (m, 14H). MS, *m/z* = 452 [M + H]⁺.

Cbz-Orn(NH₂)-Ala-Sta-NHCyhex-HCl (17). General procedure D was followed using *Cbz-Orn(N-Boc)-Ala-Sta-NHCyhex* **85** (65 mg, 0.09 mmol) to obtain **17** as a white solid (45 mg, 68%). ¹H NMR (MeOD): δ 7.36–7.31 (m, 5H), 5.12 (s, 2H), 4.35–4.30 (m, 1H), 4.20–4.10 (m, 1H), 4.00–3.85 (m, 2H), 3.69–3.60 (m, 1H), 2.98–2.90 (m, 2H), 2.31–2.23 (m, 2H), 1.90–1.15 (m, 20H), 0.95–0.92 (m, 6H). HRMS found: (M + H) 576.3751; C₃₀H₄₉N₅O₆ requires (M + H), 576.3761.

Cbz-Lys(NH₂)-Ala-Sta-NHCyhex-HCl (18). General procedure D was followed using *Cbz-Lys(N-Boc)-Ala-Sta-NHCyhex* **87** (80 mg, 0.11 mmol) to give **18** as an oil (70 mg, 96%). ¹H NMR (DMSO-*d*₆): δ 8.13–8.05 (m, 1H), 7.87 (br s, 3H), 7.63 (d, 1H, *J* 6.3 Hz), 7.50–7.41 (m, 1H), 7.35 (s, 5H), 5.04–5.02 (m, 2H), 4.87–4.79 (m, 1H), 4.57–4.41 (m, 1H), 4.05–3.90 (m, 1H), 3.99 (br s, 2H), 3.45–3.52 (m, 1H), 2.75–2.65 (m, 2H), 2.11–2.04 (m, 2H), 1.68–1.05 (m, 22H), 0.86–0.79 (m, 6H). HRMS found: (M + H) 590.3906; C₃₁H₅₁N₅O₆ requires (M + H), 590.3918.

Cbz-Arg(NH₂)-Ala-Sta-NHCyhex-TFA (19). General procedure E was followed using *Cbz-Arg(N,N-diBoc)-Ala-Sta-NHCyhex* **88** (40 mg, 34.4 mmol) to give **19** as a white solid (30 mg, 84%). ¹H NMR (DMSO-*d*₆) (rotamers): δ 8.05–7.95 (m, 1H), 7.60–7.35 (m, 2H), 7.33 (s, 5H), 5.01 (s, 2H), 4.29–4.23 (m, 1H), 4.05–3.95 (m, 1H), 3.85–3.75 (m, 1H), 3.55–3.45 (m, 1H), 3.08–3.00 (m, 2H), 2.15–2.00 (m, 2H), 1.70–1.05 (m, 20H), 1.23–1.05 (m, 6H). HRMS found: (M + H) 618.3970; C₃₁H₅₁N₇O₆ requires (M + H), 618.3979.

Cbz-hArg(NH₂)-Ala-Sta-NHCyhex-TFA (20). General procedure A was followed using *Cbz-Lys(N-Boc)-Ala-Sta-NHCyhex* **87** (30 mg, 0.036 mmol), followed by general procedure E gave **20** as a white solid (25 mg, 93%). ¹H NMR (MeOD) (rotamers): δ 7.38–7.35 (m, 5H), 5.18–5.10 (m, 2H), 4.37–4.32 (m, 1H), 4.15–3.85 (m, 3H), 3.67–3.60 (m, 1H), 3.19–3.14 (m, 2H), 2.77–2.67 and 2.31–2.24 (2 × m, 2H), 1.90–1.15 (m, 22H), 1.01–0.85 (m, 6H). HRMS found: (M + H) 632.4125; C₃₂H₅₃N₇O₆ requires (M + H), 632.4136.

Cbz-Arg(N,N-diBoc)-Ala-AHMHx-A-NHCyhex (29). General procedure D was followed using *Boc-AHMHx-A-NHCyhex* **92** to give *NH₂-AHMHx-A-NHCyhex-HCl* **25**. General procedure C was then followed using *Cbz-Arg(N,N-diBoc)-Ala-OH* **90** (50 mg, 0.086 mmol) and *NH₂-AHMHx-A-NHCyhex-HCl* **25** (28 mg, 0.01 mmol) to obtain an oil. The oil was subjected to silica chromatography gradient eluting with 100% DCM to 10% MeOH/DCM to obtain **29** as a colorless glass (30 mg, 43%). ¹H NMR (CDCl₃) (rotamers): δ 8.45–8.35 (m, 1H), 7.36 (s, 5H), 7.25–7.20 (m, 0.5H), 7.10–6.90 (m, 1H), 0.67–0.65 (m, 1H), 6.40 (br s, 0.5H), 6.25 (br s, 0.5 H), 6.10–5.95 (m, 1.5H), 5.13 (s, 2H), 4.75–4.65 (m, 1H), 4.50–4.15 (m, 2H), 3.80–3.65 (m, 1H), 3.5–3.45 (m, 3H), 2.45–2.15 (m, 2H), 1.95–1.05 (m, 36H), 0.95–0.85 (m, 6H). MS, *m/z* = 804 [M]⁺.

Cbz-Arg(N,N-diBoc)-Ala-AHMPa-A-NHCyhex (30). General procedure D was followed using *Boc-AHMPa-A-NHCyhex* **91** to give *NH₂-AHMPa-A-NHCyhex-HCl* **26**. General procedure C was then followed using *Cbz-Arg(N,N-diBoc)-Ala-OH* **90** (35 mg, 0.060 mmol) and *NH₂-AHMPa-A-NHCyhex-HCl* **26** (22 mg, 0.066 mmol) to obtain an oil. The oil was subjected to silica chromatography gradient eluting with 100% DCM to 10% MeOH/DCM to obtain **30** as a white solid (20 mg, 41%). ¹H NMR (CDCl₃) (rotamers): δ 8.44–8.36 (m, 1H), 7.36 (m, 5H), 7.10 (br s, 0.5H), 6.86 (br s, 0.5H), 6.60–6.45 (m, 1.5H), 6.35 (br s, 0.5H), 6.20 (br s, 0.5H), 6.02 br s, 0.5H), 5.14 (s, 2H), 4.50–4.20 (m, 3H), 3.80–3.65 (m, 1H), 3.60–3.35 (m, 3H), 2.35–2.15 (m, 2H), 1.95–1.05 (m, 38H), 0.97 (d, 3H, *J* 6.7 Hz), 0.86 (t, 3H, *J* 7.3 Hz). MS, *m/z* = 818 [M]⁺.

Cbz-Arg(N,N-diBoc)-Ala-AHPPa-A-NHCyhex (31). General procedure D was followed using *Boc-AHPPa-A-NHCyhex* **93** to give *NH₂-AHPPa-A-NHCyhex-HCl* **27**. General procedure C was then followed using *Cbz-Arg(N,N-diBoc)-Ala-OH* **90** (35 mg, 0.60 mmol) and *NH₂-AHPPa-A-NHCyhex-HCl* **27** (22 mg, 0.66 mmol) to obtain an oil. The oil was subjected to silica chromatography gradient eluting with 100% DCM to 10% MeOH/DCM to obtain **31** as a white solid (40 mg, 78%). MS, *m/z* = 852 [M]⁺.

Cbz-Arg(N,N-diBoc)-Ala-ACHPA-A-NHCyhex (32). General procedure D was followed using *Boc-ACHPA-A-NHCyhex* **94** to give *NH₂-ACHPA-A-NHCyhex-HCl* **28**. General procedure C was then followed using *Cbz-Arg(N,N-diBoc)-Ala-OH* **90** (44 mg, 0.75 mmol) and *NH₂-ACHPA-A-NHCyhex-HCl* **28** (25 mg, 0.75 mmol) to obtain an oil. The oil was subjected to silica chromatography gradient eluting with 100% DCM to 10% MeOH/DCM to obtain **32** as a white solid (35 mg, 54%). ¹H NMR (CDCl₃) (rotamers): δ 8.45–8.35 (m, 1H), 7.36 (5H, s), 7.20 (br s, 0.5H), 6.90–6.85 (m, 0.5H), 6.65–6.45 (m, 2.5H), 6.10–6.05 (m, 0.5H), 5.14 (s, 2H), 4.50–4.20 (m, 2H), 4.05–3.90 (m, 2H), 3.80–3.65 (m, 1H), 3.50–3.35 (m, 2H), 2.35–0.75 (m, 60H). MS, *m/z* = 858 [M]⁺.

Cbz-Arg(NH₂)-Ala-AHMHx-A-NHCyhex-TFA (33). General procedure E was followed using *Cbz-Arg(N,N-diBoc)-Ala-AHMHx-A-NHCyhex* **29** (30 mg, 0.037 mmol) to obtain **33** as a white solid (20 mg, 75%). ¹H NMR (MeOD) (rotamers): δ 7.36 (s, 5H), 5.15–5.11 (m, 2H), 4.38–4.05 (m, 3H), 3.68–3.60 (m, 1H), 3.25–3.15 (m, 2H), 2.90–2.64 (m, 2H), 2.25–2.15 (m, 1H), 2.00–1.15 (m, 17H), 1.10–0.85 (m, 6H). HRMS found: (M + H) 604.3812; C₃₀H₄₉N₇O₆ requires (M + H), 604.3823.

Cbz-Arg(NH₂)-Ala-AHMPa-A-NHCyhex-TFA (34). General procedure E was followed using *Cbz-Arg(N,N-diBoc)-Ala-AHMPa-A-NHCyhex* **30** (20 mg, 0.024 mmol) to obtain **34** as a white solid (10 mg, 56%). ¹H NMR (MeOD) (rotamers): δ 7.37 (s, 5H), 5.15–5.11 (m, 2H), 4.35–4.05 (m, 3H), 3.68–3.49 (m, 2H), 3.25–3.15 (m, 2H), 2.70–2.64 and 2.29–2.19 (2 × m, 2H), 1.90–1.10 (m, 20H), 1.03–0.97 (m, 6H). HRMS found: (M + H) 618.3969; C₃₁H₅₁N₇O₆ requires (M + H), 618.3979.

Cbz-Arg(NH₂)-Ala-AHPPa-A-NHCyhex-TFA (35). General procedure E was followed using *Cbz-Arg(N,N-diBoc)-Ala-AHPPa-A-NHCyhex* **31** (40 mg, 0.47 mmol) to obtain a white solid **35** (23 mg, 64%). ¹H NMR (MeOD): δ 7.35–7.10 (m, 10H), 5.08 (s, 2H), 4.25–3.95 (m, 3H), 3.65–3.50 (m, 1H), 3.20–3.10 (m, 2H), 2.95–2.75 (m, 2H), 2.30–2.15 (m, 2H), 1.85–1.08 (m, 17H). HRMS found: (M + H) 652.3813; C₃₄H₄₉N₇O₆ requires (M + H), 652.3823.

Cbz-Arg(NH₂)-Ala-ACHPA-NHCyhex-TFA (36). General procedure E was followed using Cbz-Arg(*N,N*-diBoc)-Ala-ACHPA-NHCyhex **32** (30 mg, 0.035 mmol) to obtain **36** as a white solid (20 mg, 89%). ¹H NMR (MeOD) (rotamers): δ 7.39–7.30 (m, 5H), 5.12 (s, 2H), 4.36–4.31 (m, 1H), 4.20–4.08 (m, 1H), 3.98–3.94 (m, 1H), 3.67–3.60 (m, 1H), 3.23–3.18 (m, 2H), 2.76–2.67 and 2.30–2.23 (2 × m, 2H), 1.90–0.80 (m, 30H). HRMS found: (M + H) 658.4283; C₃₄H₅₅N₇O₆ requires (M + H), 658.4292.

Cbz-Orn(N-Boc)-Val-OH (37). General procedure B was followed using Cbz-Orn(N-Boc)-Val-OMe **95** (195 mg, 0.41 mmol) to obtain **37** as an oil (170 mg, 90%). ¹H NMR (CDCl₃) (rotamers): δ 7.25 (5H, s), 6.34 (br s, 1H), 5.09–5.00 (m, 3H), 4.37–4.25 (m, 1H), 4.05 (br s, 1H), 3.40–2.95 (m, 2H), 2.12–2.02 (m, 1H), 1.80–1.35 (m, 13H), 0.90–0.78 (m, 6H). *m/z* = 466 [M + H]⁺.

Cbz-Orn(N-Boc)-Ile-OH (38). General procedure B was followed using Cbz-Orn(N-Boc)-Ile-OMe **96** (210 mg, 0.41 mmol) to obtain **38** as an oil (150 mg, 76%). ¹H NMR (CDCl₃) (rotamers): δ 7.30 (s, 5H), 6.27 (br s, 1H), 5.12–4.95 (m, 3H), 4.35–4.20 (m, 1H), 4.10–3.95 (m, 1H), 3.30–2.85 (m, 2H), 1.90–1.35 (m, 16H), 0.92–0.79 (m, 6H). *m/z* = 480 [M + H]⁺.

Cbz-Orn(N-Boc)-Leu-OH (40). General procedure B was followed using Cbz-Orn(N-Boc)-Leu-OMe **97** (210 mg, 0.41 mmol) to obtain **40** as an oil (190 mg, 96%). ¹H NMR (CDCl₃) (rotamers): δ 7.30 (s, 5H), 6.20 (br s, 1H), 5.15–4.99 (m, 3H), 4.25–4.10 (m, 2H), 3.10–2.65 (m, 2H), 1.85–1.35 (m, 16H), 0.90–0.75 (m, 6H). *m/z* = 480 [M + H]⁺.

Cbz-Orn(N-Boc)-Phe-OH (41). General procedure B was followed using Cbz-Orn(N-Boc)-Phe-OEt **98** (220 mg, 0.41 mmol) to obtain **41** as an oil (120 mg, 58%). ¹H NMR (CDCl₃) (rotamers): δ 7.35–7.05 (m, 11H), 5.10–4.80 (m, 3H), 4.50 (br s, 1H), 4.10–4.00 (m, 1H), 3.30–2.80 (m, 4H), 1.60–1.15 (m, 13H), *m/z* = 514 [M + H]⁺.

Cbz-Orn(N-Boc)-Val-Sta-NHCyhex (42). General procedure C was followed using Cbz-Orn(N-Boc)-Val-OH **37** (50 mg, 0.11 mmol) and HCl-NH₂-Sta-NHCyhex **6** (32 mg, 0.1 mmol) to obtain a solid. The solid was triturated with Et₂O and filtered off to obtain **42** as a white solid (45 mg, 60%). ¹H NMR (CDCl₃) (rotamers): δ 7.35 (s, 5H), 7.19 (br s, 0.5H), 6.93 (br s, 0.5H), 6.70–6.55 (m, 2H), 5.82 (br s, 1H), 5.15–5.07 (m, 2H), 4.89–4.80 (m, 1H), 4.30–4.13 (m, 2H), 4.00–3.90 (m, 2H), 3.78–3.69 (m, 1H), 3.20–3.05 (m, 2H), 2.35–1.1 (m, 18H), 0.95–0.85 (m, 12H). *m/z* = 704 [M + H]⁺.

Cbz-Orn(N-Boc)-Ile-Sta-NHCyhex (43). General procedure C was followed using Cbz-Orn(N-Boc)-Ile-OH **38** (50 mg, 0.11 mmol) and HCl-NH₂-Sta-NHCyhex **6** (32 mg, 0.1 mmol) to obtain an oil. The oil was subjected to silica chromatography gradient eluting with 100% DCM to 10% MeOH/DCM to obtain **43** as an oil (30 mg, 40%). *m/z* = 718 [M + H]⁺.

Cbz-Orn(N-Boc)-Leu-Sta-NHCyhex (44). General procedure C was followed using Cbz-Orn(N-Boc)-Leu-OH **40** (50 mg, 0.11 mmol) and HCl-NH₂-Sta-NHCyhex **6** (32 mg, 0.1 mmol) to obtain a solid. The solid was triturated with Et₂O and filtered off to obtain **44** as a white solid (65 mg, 86%). ¹H NMR (CDCl₃) (rotamers): δ 7.34 (s, 5H), 7.08 (br s, 0.5H), 6.75–6.40 (m, 1.5H), 5.85–5.80 (m, 1H), 5.12 (s, 2H), 4.95–4.80 (m, 1H), 4.45–4.30 (m, 2H), 3.98–3.85 (m, 2H), 3.75–3.65, 3.30–3.05 (m, 2H), 2.30–1.10 (m, 29H), 0.95–0.85 (m, 12H). *m/z* = 718 [M + H]⁺.

Cbz-Orn(N-Boc)-Phe-Sta-NHCyhex (45). General procedure C was followed using Cbz-Orn(N-Boc)-Phe-OH **41** (50 mg, 0.1 mmol) and HCl-NH₂-Sta-NHCyhex **6** (32 mg, 0.1 mmol) to obtain a solid. The solid was triturated with Et₂O and filtered off to obtain **45** as a white solid (25 mg, 34%). ¹H NMR (CDCl₃) (rotamers): δ 7.39–7.21 (m, 10H), 6.85–6.70 (m, 2H), 6.40–6.30 (m, 2H), 5.11–5.02 (m, 2H), 4.75–4.55 (m, 3H), 4.21–3.85 (m, 3H), 3.80–3.65 (m, 2H), 3.23–3.02 (m, 4H), 1.90–1.15 (m, 26H), 0.92–0.85 (m, 6H). *m/z* = 752 [M + H]⁺.

Cbz-Arg(NH₂)-Val-Sta-NHCyhex-TFA (46). General procedure E was followed using Cbz-Arg(*N,N*-diBoc)-Val-Sta-NHCyhex **99** (25 mg, 0.03 mmol) to obtain **46** as a white solid (17 mg, 76%). ¹H NMR (MeOD): δ 7.26 (s, 5H), 5.12 (s, 2H), 4.24–4.14 (m, 2H), 4.02–3.92 (m, 2H), 3.69–3.60 (m, 1H), 3.22–3.18 (m, 2H), 2.29–2.19 (m, 2H),

2.09–2.05 (m, 2H), 1.90–1.15 (m, 17H), 1.0–0.85 (m, 12H). HRMS found: (M + H) 646.4282; C₃₃H₅₅N₇O₆ requires (M + H), 646.4292.

Cbz-Arg(NH₂)-Ile-Sta-NHCyhex-TFA (47). General procedure E was followed using Cbz-Arg(*N,N*-diBoc)-Ile-Sta-NHCyhex **100** (55 mg, 0.064 mmol), to obtain **47** as a white solid (55 mg, 83%). ¹H NMR (MeOD): δ 7.38–7.35 (m, 5H), 5.12 (s, 2H), 4.40–4.35 (m, 1H), 4.21–4.14 (m, 1H), 4.05–3.92 (m, 2H), 3.69–3.60 (m, 1H), 3.23–3.15 (m, 2H), 2.31–2.23 (m, 2H), 1.90–1.15 (m, 20H), 0.98–0.84 (m, 12H). HRMS found: (M + H) 660.4439; C₃₄H₅₇N₇O₆ requires (M + H), 660.4449.

Cbz-Arg(NH₂)-Leu-Sta-NHCyhex-TFA (48). General procedure E was followed using Cbz-Arg(*N,N*-diBoc)-Leu-Sta-NHCyhex **101** (25 mg, 0.029 mmol) to obtain **48** as a white solid (19 mg, 85%). ¹H NMR (MeOD): δ 7.37 (s, 5H), 5.12 (s, 2H), 4.41–4.36 (m, 1H), 4.19–3.90 (m, 3H), 3.68–3.61 (m, 1H), 3.21–3.18 (m, 2H), 2.30–2.22 (m, 2H), 1.90–1.15 (m, 20H), 1.02–0.91 (m, 12H). HRMS found: (M + H) 660.4440; C₃₄H₅₇N₇O₆ requires (M + H), 660.4449.

Cbz-Arg(NH₂)-Phe-Sta-NHCyhex-TFA (49). General procedure E was followed using Cbz-Arg(*N,N*-diBoc)-Phe-Sta-NHCyhex **102** (20 mg, 0.022 mmol) to obtain **49** as a white solid (7 mg, 39%). ¹H NMR (MeOD): δ 7.35–7.25 (m, 10H), 5.15–5.04 (m, 2H), 4.69–4.62 (m, 1H), 4.12–3.90 (m, 3H), 3.68–3.61 (m, 1H), 3.25–2.85 (m, 4H), 2.29–2.04 (m, 2H), 1.90–1.15 (m, 17H), 1.01–0.84 (m, 6H). HRMS found: (M + H) 694.4285; C₃₇H₅₅N₇O₆ requires (M + H), 694.4292.

Cbz-Arg(N,N-diBoc)-Ala-Sta-OH (51). General procedure B was followed using Cbz-Arg(*N,N*-diBoc)-Ala-Sta-Oallyl **104** (800 mg, 1.0 mmol), to obtain **51** as an oil (740 mg, 98%). MS, *m/z* = 737 [M + H]⁺.

Cbz-Arg(NH₂)-Ala-Sta-NH-Bzl-TFA (52). General procedure C was followed using Cbz-Arg(*N,N*-diBoc)-Ala-Sta-OH **51** (20 mg, 0.027 mmol) and benzylamine (15 mg, 0.135 mmol) to obtain an oil. The oil was subjected to silica chromatography gradient eluting with 100% DCM to 10% MeOH/DCM to obtain Cbz-Arg(*N,N*-diBoc)-Ala-Sta-NH-Bzl **105** as an oil (14 mg, 62%). General procedure E was followed using Cbz-Arg(*N,N*-diBoc)-Ala-Sta-NH-Bzl **105** (14 mg, 0.017 mmol) to obtain a white solid **52** (9 mg, 72%). ¹H NMR (MeOD) (rotamers): δ 7.33–7.22 (m, 5H), 5.14–5.07 (m, 2H), 4.41–4.31 (m, 3H), 4.16–3.97 (m, 3H), 3.19–3.14 (m, 2H), 2.84–2.76 and 2.40–2.33 (2 × m, 2H), 1.90–1.30 (m, 10H), 1.01–0.85 (m, 6H). HRMS found: (M + H) 626.3657; C₃₂H₄₇N₇O₆ requires (M + H), 626.3666.

Cbz-Arg(NH₂)-Ala-Sta-NH(CH₂)₂Ph-TFA (53). General procedure C was followed using Cbz-Arg(*N,N*-diBoc)-Ala-Sta-OH **51** (20 mg, 0.027 mmol) and phenethylamine (17 mg, 0.14 mmol) to obtain an oil. The oil was subjected to silica chromatography gradient eluting with 100% DCM to 10% MeOH/DCM to obtain Cbz-Arg(*N,N*-diBoc)-Ala-Sta-NH(CH₂)₂Ph **106** as an oil (13 mg, 57%). General procedure E was followed using Cbz-Arg(*N,N*-diBoc)-Ala-Sta-NH(CH₂)₂Ph **106** (13 mg, 0.015 mmol) to obtain a white solid **53** (9 mg, 77%). ¹H NMR (MeOD): δ 7.60–7.20 (m, 10H), 5.12 (s, 2H), 4.36–4.28 (m, 1H), 4.18–4.08 (m, 1H), 4.00–3.91 (m, 2H), 3.45–3.35 (m, 2H), 3.21–3.17 (m, 2H), 2.83–2.78 (m, 2H), 2.32–3.23 (m, 2H), 1.85–1.30 (m, 10H), 1.01–0.89 (m, 6H). HRMS found: (M + H) 640.3812; C₃₃H₄₉N₇O₆ requires (M + H), 640.3823.

Cbz-Arg(NH₂)-Ala-Sta-NH-Indane-TFA (54). General procedure C was followed using Cbz-Arg(*N,N*-diBoc)-Ala-Sta-OH **51** (20 mg, 0.027 mmol) and 2-aminoindane (18 mg, 0.135 mmol) to obtain an oil. The oil was subjected to silica chromatography gradient eluting with 100% DCM to 10% MeOH/DCM to obtain Cbz-Arg(*N,N*-diBoc)-Ala-Sta-NH-indane **107** as an oil (18 mg, 78%). General procedure E was then followed using Cbz-Arg(*N,N*-diBoc)-Ala-Sta-NH-indane **107** (18 mg, 0.021 mmol) to obtain a white solid **54** (9 mg, 56%). ¹H NMR (MeOD) (rotamers): δ 7.36–7.12 (m, 10H), 5.14–5.06 (m, 2H), 4.62–4.55 (m, 1H), 4.35–4.25 (m, 1H), 4.15–3.85 (m, 3H), 3.30–3.15 (m, 4H), 2.90–2.80 (m, 2H), 2.76–2.67 and 2.31–2.26 (2 × m, 2H), 1.90–1.30 (m, 10H), 1.02–0.89 (m, 6H). HRMS found: (M + H) 652.3812; C₃₄H₄₉N₇O₆ requires (M + H), 652.3823.

Cbz-Arg(NH₂)-Ala-Sta-NHCH(CH₃)Ph-TFA (55). General procedure C was followed using Cbz-Arg(*N,N*-diBoc)-Ala-Sta-OH **51** (20 mg,

0.027 mmol) and 1-methylbenzylamine (16 mg, 0.135 mmol) to obtain an oil. The oil was subjected to silica chromatography gradient eluting with 100% DCM to 10% MeOH/DCM to obtain Cbz-Arg(*N,N*-diBoc)-Ala-Sta-NHCH(CH₃)Ph **108** as an oil (20 mg, 88%). General procedure E was then followed using Cbz-Arg(*N,N*-diBoc)-Ala-Sta-NHCH(CH₃)Ph **108** (20 mg, 0.024 mmol) to obtain a white solid **55** (9 mg, 50%). ¹H NMR (MeOD): δ 7.37–7.21 (m, 10H), 5.14–4.95 (m, 3H), 4.40–4.30 (m, 1H), 4.20–3.90 (m, 3H), 3.20–3.10 (m, 2H), 2.88–2.70 (m, 1H), 2.37–2.30 (m, 1H), 1.90–1.30 (m, 13H), 0.98–0.86 (m, 6H). HRMS found: (M + H) 640.3811; C₃₃H₄₉N₇O₆ requires (M + H), 640.3823.

Cbz-Arg(NH₂)-Ala-Sta-NH(CH₂)₂Ph(4'-Cl)-TFA (56). General procedure E was followed using Cbz-Arg(*N,N*-diBoc)-Ala-Sta-NH-(CH₂)₂Ph(4'-Cl) **109** (44 mg, 0.05 mmol) to afford the title compound **56** as a colorless oil (30 mg, 76% yield). ¹H NMR (300 MHz, MeOD, 325 K) δ 7.38–7.15 (m, 9H, ArH), 5.15–5.02 (m, 2H), 4.31 (d, *J* = 7.1 Hz, 1H), 4.20–4.06 (m, 1H), 3.94 (d, *J* = 6.2 Hz, 2H), 3.46–3.34 (m, 2H), 3.25–3.14 (m, 2H), 2.82–2.73 (m, 2H), 2.32–2.22 (m, 2H), 1.77–1.53 (m, 6H), 1.45–1.28 (m, 4H), 0.97–0.86 (m, 6H). HRMS found: (M + H) 674.3422; C₃₃H₄₈ClN₇O₆ requires (M + H), 674.3433.

Cbz-Arg(NH₂)-Ala-Sta-NCH₃(CH₂)₂Ph(4'-Cl)-TFA (57). General procedure E was followed using Cbz-Arg(*N,N*-diBoc)-Ala-Sta-NCH₃(CH₂)₂Ph(4'-Cl) **110** (40 mg, 0.045 mmol) to afford the title compound **57** as an oil (25 mg, 70% yield). ¹H NMR (300 MHz, MeOD): δ 7.39–7.16 (m, 9H, ArH), 5.09 (s, 2H), 4.31 (s, 1H), 4.20–3.81 (m, 3H), 3.66–3.45 (m, 2H), 3.18 (s, 2H), 3.00–2.74 (m, 5H), 2.53–2.15 (m, 2H), 1.87–1.51 (m, 6H), 1.36 (s, 4H), 0.90 (s, 6H). HRMS found: (M + H) 688.3581; C₃₄H₅₀ClN₇O₆ requires (M + H), 688.3589.

Bz-Orn(N-Boc)-Ala-OH (60). General procedure B was followed using Bz-Orn(N-Boc)-Ala-OEt **112** (170 mg, 0.64 mmol) to obtain **60** as a colorless oil (155 mg, 98%). ¹H NMR (CDCl₃): δ 7.95 (br s, 1H), 7.89–7.86 (m, 2H), 7.57 (d, 1H, *J* 6.9 Hz), 7.51–7.36 (m, 3H), 4.97–4.89 (m, 1H), 4.52–4.42 (m, 1H), 3.25–3.05 (m, 2H), 1.95–1.55 (m, 4H), 1.45–1.35 (m, 12H). *m/z* = 408 [M + H]⁺.

BzIOAc-Orn(N-Boc)-Ala-OH (61). General procedure B was followed using BzIOAc-Orn(N-Boc)-Ala-OEt **113** (170 mg, 0.64 mmol) to obtain **61** as a colorless oil (150 mg, 94%). ¹H NMR (CDCl₃): δ 7.44–7.32 (m, 5H), 4.71–4.51 (m, 4H), 3.96 (s, 2H), 3.25–3.05 (m, 2H), 1.95–1.50 (m, 4H), 1.49–1.44 (m, 12H). *m/z* = 452 [M + H]⁺.

PhSO₂-Orn(N-Boc)-Ala-OH (62). General procedure B was followed using PhSO₂-Orn(N-Boc)-Ala-OEt **111** (170 mg, 0.64 mmol) to obtain **62** as a colorless oil (155 mg, 97%). ¹H NMR (CDCl₃): δ 7.95 (br s, 1H), 7.89–7.86 (m, 2H), 7.56 (d, 1H, *J* 6.9 Hz), 7.51–7.36 (m, 3H), 4.97–4.89 (m, 1H), 4.52–4.42 (m, 1H), 3.99–3.96 (m, 1H), 3.30–3.10 (m, 2H), 2.05–1.60 (m, 4H), 1.43 (s, 12H). *m/z* = 444 [M + H]⁺.

PhCH₂SO₂-Orn(N-Boc)-Ala-OH (63). General procedure B was followed using PhCH₂SO₂-Orn(N-Boc)-Ala-OEt **114** (170 mg, 0.64 mmol) to obtain **63** as a colorless oil (155 mg, 97%). ¹H NMR (CDCl₃): δ 7.43–2.34 (m, 5H), 7.26–7.24 (m, 1H), 6.00 (br s, 1H), 4.52–4.59 (1H, m), 4.27 (s, 2H), 3.98–3.93 (m, 1H), 3.14–2.95 (m, 1H), 1.86–1.43 (m, 16H). *m/z* = 458 [M + H]⁺.

Bz-Orn(N-Boc)-Ala-Sta-NH(CH₂)₂Ph (65). General procedure C was followed using Bz-Orn(N-Boc)-Ala-OH **60** (80 mg, 0.2 mmol) and NH₂-Sta-NH(CH₂)₂Ph-HCl **116** (80 mg, 0.25 mmol) to obtain **65** as a colorless oil (70 mg, 53%). ¹H NMR (CDCl₃) (rotamers): δ 7.88–7.12 (11H, m), 6.85–6.81 (m, 1H), 6.65–6.61 (d, 1H, *J* 9.3 Hz), 5.05–4.90 (m, 1H), 4.80–4.65 (m, 1H), 4.45–4.35 (m, 1H), 4.01–3.85 (m, 2H), 3.55–3.05 (m, 4H), 2.84–2.71 (m, 2H), 2.37–2.25 (m, 2H), 2.00–1.35 (m, 19H), 0.90–0.82 (m, 6H). *m/z* = 668 [M + H]⁺.

BzIOAc-Orn(N-Boc)-Ala-Sta-NH(CH₂)₂Ph (66). General procedure C was followed using BzIOAc-Orn(N-Boc)-Ala-OH **61** (88 mg, 0.19 mmol), and NH₂-Sta-NH(CH₂)₂Ph-HCl **116** (82 mg, 0.26 mmol) to obtain **66** as a colorless oil (90 mg, 65%). ¹H NMR (CDCl₃) (rotamers): δ 7.37–7.15 (m, 10H), 7.05 (br s, 0.5H), 6.70–6.6 (m, 1H), 6.49–6.45 (m, 1H), 5.00 (br s, 0.5H), 4.84 (br s, 0.5H), 4.60–4.30 (m, 4H), 4.00–3.85 (m, 4H), 3.55–3.35 (m, 2H), 3.25–3.05 (m,

2H), 2.84–2.77 (m, 2H), 2.32–2.25 (m, 2H), 1.90–1.30 (m, 19H), 0.91–0.87 (m, 6H). *m/z* = 712 [M + H]⁺.

PhSO₂-Orn(N-Boc)-Ala-Sta-NH(CH₂)₂Ph (67). General procedure C was followed using PhSO₂-Orn(N-Boc)-Ala-OH **62** (95 mg, 0.2 mmol) and NH₂-Sta-NH(CH₂)₂Ph-HCl **116** (82 mg, 0.26 mmol) to obtain **67** as a colorless oil (95 mg, 64%). ¹H NMR (CDCl₃) (rotamers): δ 7.90–7.88 (m, 2H), 7.58–7.15 (m, 9H), 7.05 (br s, 0.5H), 6.88–6.76 (m, 2H), 6.58 (d, 0.5H, *J* 7.2 Hz), 4.95–4.85 (m, 1H), 4.45–4.35 (m, 0.5H), 4.23–4.15 (m, 0.5H), 4.05–3.85 (m, 3H), 3.55–3.35 (m, 2H), 3.20–2.85 (m, 2H), 2.84–2.74 (m, 2H), 2.35–2.27 (m, 2H), 1.70–1.25 (m, 19H), 0.92–0.86 (m, 6H). *m/z* = 704 [M + H]⁺.

PhCH₂SO₂-Orn(N-Boc)-Ala-Sta-NH(CH₂)₂Ph (68). General procedure C was followed using PhCH₂SO₂-Orn(N-Boc)-Ala-OH **63** (90 mg, 0.18 mmol) and NH₂-Sta-NH(CH₂)₂Ph-HCl **116** (76 mg, 0.24 mmol) to obtain **68** as a colorless oil (80 mg, 58%). ¹H NMR (CDCl₃) (rotamers): δ 7.40–7.15 (m, 10H), 6.91–6.68 (m, 2H), 6.10–5.99 (m, 1H), 4.95–4.85 (m, 1H), 4.45–4.30 (m, 1H), 4.29–2.25 (m, 2H), 3.95–3.80 (m, 3H), 3.55–3.25 (m, 2H), 3.25–2.95 (m, 2H), 2.81–2.73 (m, 2H), 2.30–2.20 (m, 2H), 1.20–1.30 (19H, m), 0.90–0.87 (m, 6H). *m/z* = 718 [M + H]⁺.

Bz-Arg(NH₂)-Ala-Sta-NH(CH₂)₂Ph-TFA (70). General procedure A was followed using Bz-Arg(*N,N*-diBoc)-Ala-Sta-NH(CH₂)₂Ph **118** (40 mg, 0.05 mmol) to obtain **70** as a white solid (40 mg, 84%). ¹H NMR (MeOD) (rotamers): δ 7.92–7.88 (m, 2H), 7.58–7.45 (m, 3H), 7.29–7.18 (m, 5H), 4.60–4.41 (m, 3H), 4.00–3.90 (m, 2H), 3.42–3.34 (m, 2H), 3.27–3.23 (m, 2H), 2.83–2.75 (m, 2H), 2.65–2.60 and 2.35–2.27 (2 × m, 2H), 2.00–1.30 (m, 10H), 1.01–0.77 (m, 6H). HRMS found: (M + H) 610.3707; C₃₂H₄₇N₇O₅ requires (M + H), 610.3717.

BzIOAc-Arg(NH₂)-Ala-Sta-CONH(CH₂)₂Ph-TFA (71). General procedure A was followed using BzIOAc-Arg(*N,N*-diBoc)-Ala-Sta-NH-(CH₂)₂Ph **119** (30 mg, 0.035 mmol) to obtain **71** as a white solid (21 mg, 78%). ¹H NMR (MeOD) (rotamers): δ 7.39–7.18 (m, 10H), 4.63 (s, 2H), 4.50–4.25 (m, 2H), 4.05–3.85 (m, 2H), 3.45–3.35 (m, 2H), 3.25–3.15 (m, 2H), 2.80–2.75 (m, 2H), 2.70–2.65 and 2.31–2.24 (2 × m, 2H), 1.95–1.30 (m, 10H), 1.01–0.88 (m, 6H). HRMS found: (M + H) 654.3970; C₃₄H₅₁N₇O₆ requires (M + H), 654.3979.

PhCH₂SO₂-Arg(NH₂)-Ala-Sta-NH(CH₂)₂Ph-TFA (72). General procedure A was followed using PhCH₂SO₂-Arg(*N,N*-diBoc)-Ala-Sta-NH(CH₂)₂Ph **120** (40 mg, 0.05 mmol) to obtain **72** as a white solid (25 mg, 69%). ¹H NMR (MeOD): δ 7.44–7.19 (m, 10H), 4.40–4.29 (m, 3H), 3.99–3.55 (m, 3H), 3.44–3.38 (m, 1H), 3.20–3.12 (m, 2H), 2.83–2.76 (m, 2H), 2.75–2.71 and 2.28–2.24 (2 × m, 2H), 1.01–0.85 (m, 6H). HRMS found: (M + H) 660.3536; C₃₂H₄₉N₇O₆S requires (M + H), 660.3543.

PhSO₂-Arg(NH₂)-Ala-Sta-NH(CH₂)₂Ph-TFA (73). General procedure A was followed using PhSO₂-Arg(*N,N*-diBoc)-Ala-Sta-NH(CH₂)₂Ph **117** (40 mg, 0.05 mmol) to obtain **73** as a white solid (30 mg, 84%). ¹H NMR (MeOD): 7.92–7.85 (m, 2H), 7.66–7.53 (m, 3H), 7.31–7.20 (m, 5H), 4.15–3.75 (m, 4H), 3.44–3.40 (m, 2H), 3.13–3.06 (m, 2H), 2.83–2.77 (m, 2H), 2.29–2.19 (m, 2H), 1.75–1.21 (m, 10H), 1.01–0.87 (m, 6H). HRMS found: (M + H) 646.3381; C₃₁H₄₇N₇O₆S requires (M + H), 646.3387.

Cbz-hPhe-Ala-Sta-NHCyhex (75). General procedure D was followed using Boc-hPhe-Ala-Sta-NHCyhex **123** (120 mg, 0.2 mmol) to obtain HCl·NH₂-hPhe-Ala-Sta-NHCyhex **124** as a white solid (100 mg, 93%). A mixture of HCl·NH₂-hPhe-Ala-Sta-NHCyhex **124** (90 mg, 0.17 mmol), Et₃N (48 μL, 0.34 mmol), and Cbz-O-succinimide (45 mg, 0.18 mmol) in THF (5 mL) was allowed to stir for 18 h at 25 °C. Then 10% citric acid solution was added to the reaction mixture. The solution was extracted with EtOAc (2 × 15 mL). The organic layer was then washed with 10% NaHCO₃ solution (1 × 15 mL). The organic layer was dried (MgSO₄), and the organic layer was concentrated in vacuo to obtain an oil. The oil was subjected to silica chromatography gradient eluting with 100% DCM to 5% MeOH/DCM to obtain **75** as a white solid (90 mg, 84%). ¹H NMR (CDCl₃) (rotamers): δ 7.35–7.15 (m, 10H), 7.05 (br s, 0.5H), 6.82 (br s, 0.5H), 6.61 (br s, 0.5H), 6.54 (br s, 0.5H), 6.42 (br s, 0.5H), 6.28 (br s, 0.5H), 5.75 (br s, 0.5H), 5.55 (br s, 0.5H), 5.18–5.10 (m,

2H), 4.55–4.40 (m, 1H), 4.25–4.15 (m, 1H), 4.05–3.90 (m, 2H), 3.75–3.65 (m, 1H), 2.70–2.65 (m, 2H), 2.33–1.05 (m, 20H), 0.91–0.85 (m, 6H). $m/z = 623$ $[M]^+$.

Cbz-Orn(N-Boc)-Ala-OEt (76). A mixture of Cbz-Orn(N-Boc)-OH **8** (3.4 g, 9.3 mmol) and CDI (1.5 g, 9.3 mmol) in THF (30 mL) was stirred for 40 min. HCl-NH₂-Ala-OEt (1.71 g, 11.1 mmol) was desalted with Et₃N (1.6 mL, 11.1 mmol) in THF (20 mL) and added to the above solution. The mixture was allowed to stir for 18 h at 20 °C. The mixture was partitioned between brine and EtOAc. The layers were separated and the organic layer washed with 10% NaHCO₃ solution (30 mL), 10% citric acid solution (30 mL) and brine (30 mL). The organic layer was dried (MgSO₄) and concentrated in vacuo to give a solid. The solid was triturated with TBME and filtered off to obtain **76** as a white solid (3.1 g, 72%). ¹H NMR (CDCl₃): δ 7.34 (s, 5H), 6.82 (br s, 1H), 5.49 (br s, 1H), 5.10 (s, 2H), 4.72 (br s, 1H), 4.55–4.42 (s, 1H), 4.37 (br s, 1H), 4.22–4.13 (m, 2H), 3.34 (br s, 1H), 3.07 (br s, 1H), 2.09–1.85 (m, 2H), 1.65–1.42 (m, 2H), 1.43–1.40 (m, 12H), 1.26 (t, 3H, J 7.1 Hz). MS, $m/z = 466$ $[M + H]^+$.

General Procedure A. Ac-Arg(N,N-diBoc)-Ala-OEt (77). A mixture of Ac-Orn(N-Boc)-Ala-OEt **9** (1.5 g, 4.02 mmol) in 4 N HCl in dioxane was allowed to stir for 15 min at 20 °C. The reaction mixture was concentrated to dryness in vacuo. The residue was dissolved in dichloromethane (15 mL), and Et₃N (1.8 mL, 12.9 mmol) was added. The solution was stirred vigorously for 5 min. *N,N'*-Bis-Boc-1-guanylpiperazine (551 mg, 1.78 mmol) was added, and the solution was left to stir for 12 h. Citric acid solution was added to the reaction mixture. The solution was extracted with DCM (2 \times 15 mL). The organic layer was then washed with 10% NaHCO₃ solution (1 \times 20 mL). The organic layer was dried (MgSO₄), and the organic layer was concentrated in vacuo to obtain an oil. The oil was subjected to silica chromatography gradient eluting with 100% DCM to 10% MeOH/DCM to obtain **77** as a colorless foam (600 mg, 72%). ¹H NMR (CDCl₃): δ 11.49 (s, 1H), 8.46–8.40 (m, 1H), 7.43 (d, 1H, J 8.2 Hz), 6.79 (d, 1H, J 7.2 Hz), 4.56–4.46 (m, 2H), 4.19 (q, 2H, J 7.1 Hz), 3.65–3.53 (m, 1H), 3.35–3.27 (m, 1H), 2.08 (s, 3H), 1.92–1.66 (m, 4H), 1.49 (s, 18H), 1.38 (d, 3H, J 7.2 Hz), 1.29 (t, 3H, J 7.1 Hz). MS, $m/z = 516$ $[M + H]^+$.

General Procedure C. Fmoc-Sta-Ala-NH₂ (78). A mixture of Fmoc-Sta-OH **2** (50 mg, 0.126 mmol), Et₃N (43 μ L, 0.503 mmol), alaninamide-HCl (21 mg, 0.164 mmol), and HBTU (62 mg, 0.164 mmol) in DMF (0.2 mL) was allowed to stir for 18 h at 20 °C. Citric acid solution was added to the reaction mixture. The solution was extracted with EtOAc (2 \times 10 mL). The organic layer was then washed with 10% NaHCO₃ solution (1 \times 10 mL). The organic layer was dried (MgSO₄), and the organic layer was concentrated in vacuo to obtain an oil. The oil obtained was subjected to silica chromatography gradient eluting with 100% DCM to 10% MeOH/DCM to obtain **78** as a colorless oil (50 mg, 85%). ¹H NMR (CDCl₃): δ 7.74 (d, 2H, J 9.0 Hz), 7.56 (d, 2H, J 7.3 Hz), 7.40–7.26 (m, 4H), 7.08 (d, 1H, J 7.5 Hz), 6.62 (s, 1H), 6.00 (s, 1H), 5.18 (d, 1H, J 9.9 Hz), 4.48–4.38 (m, 2H), 4.22–4.16 (m, 2H), 3.95 (br s, 1H), 3.62 (br s, 1H), 2.37–2.33 (m, 1H), 1.99–1.97 (m, 1H), 1.59–1.51 (m, 2H), 1.36–1.33 (m, 4H), 0.90–0.86 (m, 6H).

Fmoc-Sta-NH(CH₂)₃CONH₂ (79). General procedure C was followed using Fmoc-Sta-OH **2** (120 mg, 0.3 mmol) and 4-aminobutyric acid amide hydrochloride (50 mg, 0.36 mmol) to obtain a crude gum. The gum was triturated with Et₂O and filtered off, washing with Et₂O to obtain **79** as a white solid (140 mg, 96%). ¹H NMR (CDCl₃): δ 7.74 (d, 2H, J 7.5 Hz), 7.57 (d, 2H, J 7.4 Hz), 7.38–7.26 (m, 4H), 6.81–6.77 (m, 1H), 6.27 (br s, 1H), 5.84 (br s, 1H), 5.19 (d, 1H, J 9.9 Hz), 4.48–4.31 (m, 3H), 4.18 (m, 1H), 3.66–3.60 (m, 1H), 3.31–3.23 (m, 2H), 2.30–2.19 (m, 4H), 1.84–1.84 (m, 2H), 1.62–1.50 (m, 2H), 1.34–1.29 (m, 1H), 0.90–0.86 (m, 6H).

Boc-Sta-NHCyhex (80). General procedure C was followed using Boc-Sta-OH **3** (500 mg, 1.82 mmol) and cyclohexylamine (620 μ L, 4.54 mmol) to obtain a gum. The gum was subjected to column chromatography eluting 100% DCM to 7% MeOH/DCM to obtain **80** as a white solid (600 mg, 93%). ¹H NMR (CDCl₃): δ 5.88 (d, 1H, J 6.7 Hz), 4.74 (d, 1H, J 9.7 Hz), 4.24 (s, 1H), 3.97–3.94 (1H, m), 3.80–3.70 (m, 1H), 3.61–3.53 (m, 1H), 3.27–3.20 (m, 1H), 2.42–

2.20 (m, 2H), 1.91–1.19 (m, 22H), 0.90–0.86 (m, 6H). MS, $m/z = 357$ $[M + H]^+$, 713 $[2M + H]^+$.

Ac-Arg(N,N-diBoc)-Ala-Sta-Ala-NH₂ (81). A mixture of Fmoc-Sta-Ala-NH₂ **78** (150 mg, 0.32 mmol) and piperidine (0.2 mL) in DMF (0.5 mL) was allowed to stir for 30 min at 20 °C. The reaction mixture was concentrated to dryness in vacuo. The oil obtained was subjected to silica chromatography gradient eluting with 100% dichloromethane to 20% methanol/dichloromethane to obtain NH₂-Sta-Ala-NH₂ **4** as a white solid (65 mg, 82%). General procedure C was then followed using Ac-Arg(N,N-diBoc)-Ala-OH **10** (50 mg, 0.103 mmol) and NH₂-Sta-Ala-NH₂ **4** (25 mg, 0.102 mmol) to obtain an oil. The oil was subjected to silica chromatography gradient eluting with 100% DCM to 10% MeOH/DCM to obtain **81** as a colorless oil (35 mg, 48%). MS, $m/z = 715$ $[M + H]^+$.

Ac-Arg(N,N-diBoc)-Ala-Sta-NH(CH₂)₃CONH₂ (83). A mixture of Fmoc-Sta-NH(CH₂)₃CONH₂ **79** (140 mg, 0.29 mmol) and piperidine (575 μ L, 5.8 mmol) in tetrahydrofuran (2 mL) was allowed to stir for 1 h at 20 °C. The reaction mixture was concentrated to dryness in vacuo. The solid was triturated with Et₂O and decanted off (repeated 3 times). The resulting solid NH₂-Sta-NH(CH₂)₃CONH₂ **82** was used in the next reaction without further purification. General procedure C was then followed using Ac-Arg(N,N-diBoc)-Ala-OH **10** (50 mg, 0.103 mmol) and **82** (32 mg, 0.12 mmol) to obtain an oil. The oil was subjected to silica chromatography gradient eluting with 100% DCM to 12% MeOH/DCM to obtain **83** as a colorless oil (20 mg, 27%). MS, $m/z = 729$ $[M + H]^+$.

Ac-Arg(N,N-diBoc)-Ala-Sta-NHCyhex (84). General procedure C was followed using Ac-Arg(N,N-diBoc)-Ala-OH **10** (30 mg, 0.06 mmol) and HCl-NH₂-Sta-NHCyhex **6** (27 mg, 0.074 mmol) to obtain an oil. The oil was subjected to silica chromatography gradient eluting with 100% DCM to 10% MeOH/DCM to obtain **84** as a colorless oil (25 mg, 56%). MS, $m/z = 726$ $[M + H]^+$.

Cbz-Orn(N-Boc)-Ala-Sta-NHCyhex (85). General procedure C was followed using Cbz-Orn(N-Boc)-Ala-OH **15** (45 mg, 0.10 mmol) and (60 mg, 0.20 mmol) to obtain an oil. The oil was subjected to silica chromatography gradient eluting with 100% DCM to 10% MeOH/DCM to obtain **85** as a colorless oil (65 mg, 93%). MS, $m/z = 676$ $[M + H]^+$.

Cbz-Lys(N-Boc)-Ala-OEt (86). A mixture of Cbz-Lys(N-Boc)-OH **14** (2.5 g, 6.6 mmol) and CDI (1.07 g, 6.57 mmol) in THF (30 mL) was stirred for 40 min. HCl-NH₂-Ala-OEt (1.21 g, 7.89 mmol) was desalted with Et₃N (1.1 mL, 7.89 mmol) in THF (20 mL) and added to the above solution. The mixture was allowed to stir for 18 h at 20 °C. The mixture was partitioned between brine and EtOAc. The layers were separated and the organic layer washed with 10% NaHCO₃ solution (30 mL), 10% citric acid solution (30 mL), and brine (30 mL). The organic layer was dried (MgSO₄) and concentrated in vacuo to give a solid. The solid was triturated with TBME and filtered off to obtain **86** as a white solid (2.79 g, 89%). ¹H NMR (CDCl₃): δ 7.36 (s, 5H), 6.57 (br s, 1H), 5.12 (s, 2H), 4.69 (br s, 1H), 4.60–4.50 (m, 1H), 4.21 (q, 2H, J 7.2 Hz), 3.14–3.08 (2H, m), 1.92–1.85 (m, 2H), 1.71–1.64 (m, 2H), 1.55–1.40 (m, 14H), 1.29 (t, 3H, J 7.1 Hz). MS, $m/z = 480$ $[M + H]^+$.

Cbz-Lys(N-Boc)-Ala-Sta-NHCyhex (87). General procedure C was followed using Cbz-Lys(N-Boc)-Ala-OH **16** (100 mg, 0.221 mmol), and HCl-NH₂-Sta-NHCyhex **6** (77.8 mg, 0.27 mmol) to obtain an oil. The oil was subjected to silica chromatography gradient eluting with 100% DCM to 10% MeOH/DCM to obtain **87** as a white solid (98 mg, 64%). ¹H NMR (CDCl₃) (rotamers): δ 7.31 (s, 5H), 7.07–6.70 (m, 3H), 6.16–6.06 (m, 1H), 5.14 (s, 2H), 4.87–4.79 (m, 1H), 4.57–4.41 (m, 1H), 4.20–4.05 (m, 1H), 3.99–3.95 (m, 2H), 3.74–3.67 (m, 1H), 3.10–3.00 (m, 2H), 2.29–2.26 (m, 2H), 1.90–1.14 (m, 31H), 0.90–0.86 (m, 6H). MS, $m/z = 690$ $[M + H]^+$.

Cbz-Arg(N,N-diBoc)-Ala-Sta-NHCyhex (88). General procedure A was followed using Cbz-Orn(N-Boc)-Ala-Sta-NHCyhex **85** (50 mg, 0.086 mmol) to obtain **88** as a colorless oil (45 mg, 64%). ¹H NMR (CDCl₃) (rotamers): δ 8.45–8.35 (m, 1H), 7.33 (s, 5H), 7.40 (br s, 0.5H), 6.70–6.40 (m, 2H), 6.05 (br s, 0.5H), 5.11 (s, 2H), 4.50–4.30 (m, 2H), 4.25–4.15 (m, 1H), 3.95–3.85 (m, 2H), 3.75–3.65 (m, 1H),

3.45–3.35 (m, 2H), 2.30–2.05 (m, 2H), 1.95–1.05 (m, 38H), 0.90–0.85 (m, 6H). MS, m/z = 818 $[M]^+$.

Cbz-Arg(N,N-diBoc)-Ala-OEt (89). General procedure E was followed using Cbz-Orn(N-Boc)-Ala-OEt **76** (500 mg, 1.0 mmol) to obtain **89** as a colorless foam (600 mg, 92%). ^1H NMR (CDCl_3): δ 8.36 (br s, 1H), 7.35 (s, 5H), 6.63 (br s, 1H), 5.90 (br s, 1H), 5.13 (s, 2H), 4.51–4.49 (m, 1H), 4.30–4.15 (m, 3H), 3.50–3.35 (m, 2H), 1.95–1.60 (m, 4H), 1.49 (s, 18H), 1.39 (d, 3H, J 7.1 Hz), 1.27 (t, 3H, J 7.1 Hz).

Cbz-Arg(N,N-diBoc)-Ala-OH (90). General procedure B was followed using Cbz-Arg(N,N-diBoc)-Ala-OEt **89** (225 mg, 0.37 mmol) to obtain **90** as a colorless oil (190 mg, 89%). ^1H NMR (CDCl_3): δ 8.45 (br s, 1H), 7.35 (s, 5H), 6.63 (br s, 1H), 6.00 (br s, 1H), 5.13 (s, 2H), 4.51–4.49 (m, 1H), 4.35–4.15 (m, 1H), 3.45–3.25 (m, 2H), 1.95–1.60 (m, 4H), 1.47–1.37 (m, 21H). MS, m/z = 580 $[M + H]^+$.

Boc-AHMHpA-NHCyhex (91). Boc-AHMHpA-OH-DCHA **22** (125 mg, 0.27 mmol) was desalted using 10% citric acid solution. The crude material was subjected to general procedure C using cyclohexylamine (62 μL , 0.055 mmol) to obtain **91** as an oil (95 mg, 97%). ^1H NMR (CDCl_3): δ 6.09 (d, 1H, J 7.8 Hz), 4.94 (d, 1H, J 10.1 Hz), 4.25–4.18 (m, 1H), 3.80–3.65 (m, 1H), 3.17 (t, 1H, J 10.0 Hz), 2.43–2.35 (m, 1H), 2.24–2.18 (m, 1H), 1.90–1.10 (m, 22H), 0.95–0.85 (m, 6H). MS, m/z = 357 $[M + H]^+$.

Boc-AHMHxA-NHCyhex (92). Boc-AHMHxA-OH-DCHA **21** (200 mg, 0.45 mmol) was desalted using 10% citric acid solution. The crude material was subjected to general procedure C using cyclohexylamine (103 μL , 0.9 mmol) to obtain **92** as a white solid (140 mg, 90%). ^1H NMR (CDCl_3): δ 5.93 (d, 1H, J 7.9 Hz), 4.93 (d, 1H, J 10.0 Hz), 4.24–4.20 (m, 1H), 3.81–3.72 (m, 1H), 3.13–3.07 (m, 1H), 2.45–2.37 (m, 1H), 2.23–2.17 (m, 1H), 1.95–1.10 (m, 20H), 0.98–0.96 (m, 6H). MS, m/z = 343 $[M + H]^+$.

Boc-AHPPA-NHCyhex (93). General procedure C was followed using Boc-AHPPA-OH **23** (200 mg, 0.65 mmol) using cyclohexylamine (148 μL , 0.64 mmol) to obtain **93** as a white solid (250 mg, 99%). ^1H NMR (CDCl_3): δ 7.32–7.20 (m, 5H), 5.65–5.55 (m, 1H), 5.01 (d, 1H, J 9.5 Hz), 3.96 (d, 1H, J 8.4 Hz), 3.75–3.67 (m, 2H), 3.02–2.85 (m, 2H), 2.48–2.40 (m, 1H), 2.15–2.06 (m, 1H), 1.93–1.10 (m, 19H). MS, m/z = 391 $[M + H]^+$.

Boc-ACHPA-NHCyhex (94). General procedure C was followed using Boc-ACHPA-OH **24** (100 mg, 0.32 mmol) using cyclohexylamine (73 μL , 0.63 mmol) to obtain **94** as a white solid (125 mg, 99%). ^1H NMR (CDCl_3): δ 5.97–5.90 (br s, 1H), 4.76 (d, 1H, J 10.1 Hz), 3.99–3.95 (m, 1H), 3.83–3.72 (m, 1H), 3.63–3.57 (m, 1H), 2.48–2.40 (m, 1H), 2.29–2.22 (m, 1H), 1.90–0.85 (m, 31H).

Cbz-Orn(N-Boc)-Val-OMe (95). General procedure C was followed using Cbz-Orn(N-Boc)-OH **8** (200 mg, 0.546 mmol) and $\text{HCl}\cdot\text{NH}_2\cdot\text{Val-OMe}$ (183 mg, 1.1 mmol). Then 10% citric acid solution was added to the reaction mixture. The precipitate that formed was filtered off, successively washing with water, a solution of 10% NaHCO_3 , and water to obtain **95** as a white solid (225 mg, 86%). ^1H NMR (CDCl_3): δ 7.35 (s, 5H), 6.67 (br s, 1H), 5.45 (br s, 1H), 5.13 (s, 2H), 4.65 (br s, 1H), 4.54–4.50 (m, 1H), 4.37 (br s, 1H), 3.74 (s, 3H), 3.35–3.05 (m, 2H), 2.25–2.15 (m, 1H), 1.97–1.50 (m, 4H), 1.45 (s, 9H), 0.95–0.91 (m, 6H). MS, m/z = 480 $[M + H]^+$.

Cbz-Orn(N-Boc)-Ile-OMe (96). General procedure C was followed using Cbz-Orn(N-Boc)-OH **8** (200 mg, 0.546 mmol) and $\text{HCl}\cdot\text{NH}_2\cdot\text{Ile-OMe}$ (214 mg, 1.1 mmol) to obtain **96** as a colorless oil (275 mg, 98%). ^1H NMR (CDCl_3): δ 7.36 (s, 5H), 6.65 (br s, 1H), 5.50 (br s, 1H), 5.13 (s, 2H), 4.69 (br s, 1H), 4.58–4.53 (m, 1H), 4.35 (br s, 1H), 3.73 (s, 3H), 3.32–3.05 (m, 2H), 1.93–1.88 (m, 2H), 1.67–1.1 (m, 14H), 0.95–0.89 (m, 6H). m/z = 494 $[M + H]^+$.

Cbz-Orn(N-Boc)-Leu-OMe (97). General procedure C was followed using Cbz-Orn(N-Boc)-OH **8** (200 mg, 0.546 mmol), and $\text{HCl}\cdot\text{NH}_2\cdot\text{Leu-OMe}$ (214 mg, 1.1 mmol), to obtain **97** as a colorless oil (275 mg, 98%). ^1H NMR (CDCl_3): δ 7.36 (s, 5H), 6.79 (br s, 1H), 5.53 (br s, 1H), 5.12 (s, 2H), 4.74 (br s, 1H), 4.61–4.53 (m, 1H), 4.45 (br s, 1H), 3.72 (s, 3H), 3.40–3.05 (m, 2H), 1.95–1.50 (m, 7H), 1.45 (s, 9H), 0.97–0.92 (m, 6H). m/z = 494 $[M + H]^+$.

Cbz-Orn(N-Boc)-Phe-OEt (98). General procedure C was followed using Cbz-Orn(N-Boc)-OH **8** (200 mg, 0.546 mmol) and the $\text{HCl}\cdot\text{NH}_2\cdot\text{Phe-OEt}$ (251 mg, 1.1 mmol). Then 10% citric acid solution was added to the reaction mixture. The precipitate that formed was filtered off, successively washing with water, a solution of 10% NaHCO_3 , and water to obtain **98** as a white solid (290 mg, 97%). ^1H NMR (CDCl_3): δ 7.36–7.14 (m, 10H), 6.75 (br s, 1H), 5.42 (br s, 1H), 5.11 (s, 2H), 4.84–4.77 (m, 1H), 4.69 (br s, 1H), 4.28 (br s, 1H), 4.17 (q, 2H, J 7.2 Hz), 3.25–3.02 (m, 4H), 1.87–1.45 (m, 13H), 1.25 (t, 3H, J 7.3 Hz). m/z = 542 $[M + H]^+$.

Cbz-Arg(N,N-diBoc)-Val-Sta-NHCyhex (99). General procedure A was followed using Cbz-Orn(N-Boc)-Val-Sta-NHCyhex **42** (30 mg, 0.042 mmol) to obtain **99** as a colorless oil (25 mg, 70%). m/z = 846 $[M]^+$.

Cbz-Arg(N,N-diBoc)-Ile-Sta-NHCyhex (100). General procedure A was followed using Cbz-Orn(N-Boc)-Ile-Sta-NHCyhex **43** (30 mg, 0.042 mmol), to obtain **100** as a colorless oil (30 mg, 84%). m/z = 860 $[M]^+$.

Cbz-Arg(N,N-diBoc)-Leu-Sta-NHCyhex (101). General procedure A was followed using Cbz-Orn(N-Boc)-Leu-Sta-NHCyhex **44** (30 mg, 0.042 mmol) to obtain **101** as a colorless oil (30 mg, 84%). m/z = 860 $[M]^+$.

Cbz-Arg(N,N-diBoc)-Phe-Sta-NHCyhex (102). General procedure A was followed using Cbz-Orn(N-Boc)-Phe-Sta-NHCyhex **45** (25 mg, 0.033 mmol) to obtain **102** as a colorless oil (25 mg, 84%). m/z = 894 $[M]^+$.

Boc-Sta-OAllyl (103). A mixture of Boc-Sta-OH **3** (500 mg, 1.8 mmol), K_2CO_3 (301 mg, 2.2 mmol), and allyl bromide (236 μL , 2.7 mmol) in DMF (4 mL) was allowed to stir for 2 h at 25 °C. Then 10% citric acid solution was added to the reaction mixture and the solution was extracted with EtOAc (2×20 mL). The organic layer was then washed successively with 10% NaHCO_3 solution (2×10 mL) and water (1×10 mL). The organic layer was dried (MgSO_4), and the organic layer was concentrated in vacuo to obtain **103** as an oil (500 mg, 87%). ^1H NMR (CDCl_3): δ 6.00–5.87 (m, 1H), 5.38–5.36 (m, 2H), 4.72–4.63 (m, 3H), 4.08–4.03 (m, 1H), 3.65–3.60 (m, 1H), 2.60–2.56 (m, 2H), 1.72–1.28 (m, 12H), 0.95 (d, 6H, J 6.6 Hz).

Cbz-Arg(N,N-diBoc)-Ala-Sta-OAllyl (104). General procedure D was followed using Boc-Sta-OAllyl **103** (500 mg, 1.74 mmol). $\text{NH}_2\cdot\text{Sta-OAllyl-HCl}$ **50** was obtained and used directly in the following reaction. General procedure C was then followed using $\text{NH}_2\cdot\text{Sta-OAllyl-HCl}$ **50** (850 mg, 1.47 mmol) and Cbz-Arg(N,N-diBoc)-Ala-OH **90** (388 mg, 0.75 mmol) to obtain an oil. The oil was subjected to silica chromatography gradient eluting with 100% DCM to 10% MeOH/DCM to obtain **104** as a white solid (825 mg, 72%). ^1H NMR (CDCl_3): δ 8.45 (br s, 1H), 7.36 (s, 5H), 6.85–6.65 (m, 1H), 6.50–6.35 (m, 1H), 5.95–5.85 (m, 1H), 5.35–5.20 (m, 1H), 5.14 (s, 2H), 4.62–4.60 (m, 2H), 4.45–4.15 (m, 2H), 4.10–3.95 (m, 2H), 3.45–3.35 (m, 3H), 2.52–2.48 (m, 2H), 1.75–1.30 (m, 28H), 0.92 (d, 6H, J 6.2 Hz). MS, m/z = 777 $[M + H]^+$.

Cbz-Arg(N,N-diBoc)-Ala-Sta-NH(CH₂)₂Ph(4'-Cl) (109). General procedure C was followed using Cbz-Arg(N,N-diBoc)-Ala-Sta-OH **51** (20 mg, 0.027 mmol) and 2-(4-chlorophenyl)-ethylamine (18 mg, 0.135 mmol) to obtain to give **109** as yellow oil (58 mg, 64% yield). ^1H NMR (300 MHz, CDCl_3) δ 11.41 (s, 1H), 8.39–8.29 (m, 1H), 7.34–7.27 (m, 5H), 7.25–7.18 (m, 2H), 7.13–7.05 (m, 2H), 6.98–6.74 (m, 1H), 6.71–6.46 (m, 1H), 6.40–5.98 (m, 1H), 5.13–4.97 (m, 2H), 4.49–4.10 (m, 3H), 4.00–3.83 (m, 2H), 3.51–3.28 (m, 4H), 2.82–2.68 (m, 2H), 2.31–2.18 (m, 2H), 1.89–1.54 (m, 6H), 1.49–1.44 (m, 17H), 1.35 (d, J = 5.7 Hz, 4H), 0.89 (d, J = 3.2 Hz, 3H), 0.87 (d, J = 3.4 Hz, 3H). MS, m/z = 874.6 $[M + H]^+$.

Cbz-Arg(N,N-diBoc)-Ala-Sta-NCH₂(CH₂)₂Ph(4'-Cl) (110). General procedure C was followed using Cbz-Arg(N,N-diBoc)-Ala-Sta-OH **51** (20 mg, 0.027 mmol) and 2-(4-chlorophenyl)-*N*-methylethanamine (19 mg, 0.135 mmol) to obtain to give **110** as yellow oil (53 mg, 64% yield). ^1H NMR (300 MHz, CDCl_3 , 325 K, rotamers) δ 11.43 (br s, 1H), 8.58–8.26 (m, 1H), 7.37–7.24 (m, 7H), 7.17–7.05 (m, 2H), 6.82–6.68 (m, 1H), 6.44–6.29 (m, 1H), 6.11–5.76 (m, 1H), 5.20–5.01 (m, 2H), 4.49–3.69 (m, 5H), 3.63–3.29 (m, 4H), 2.99–2.71 (m, 5H), 2.44–2.09 (m, 2H), 1.95–1.55 (m, 6H), 1.54–1.43 (m, 18H),

1.42–1.31 (m, 4H), 0.93 (d, $J = 5.8$ Hz, 6H). MS, $m/z = 888.5$ [$M + H$] $^+$.

General Procedure F. PhSO₂-Orn(N-Boc)-Ala-OEt (111). Cbz-Orn(N-Boc)-Ala-OEt **58** (300 mg, 0.64 mmol) and Pd/C in EtOAc under a hydrogen atmosphere was allowed to stir for 18 h. The mixture was filtered through Celite and concentrated to dryness in vacuo. To the crude oil was dissolved in DCM (2 mL), benzenesulfonyl chloride (89 μ L, 0.70 mmol) and Et₃N (97 μ L, 0.70 mmol) was added. The mixture was then allowed to stir for 18 h at 25 °C. The reaction mixture was concentrated to dryness in vacuo. The oil was subjected to silica chromatography gradient eluting with 100% DCM to 5% MeOH/DCM to obtain **111** as a white solid (240 mg, 80%). ¹H NMR (CDCl₃): δ 7.87–7.84 (m, 2H), 7.57–7.43 (m, 3H), 6.93 (d, 1H, J 7.6 Hz), 5.89 (d, 1H, J 8.8 Hz), 4.87 (s, 1H), 4.37–3.99 (m, 4H), 3.30–2.95 (m, 2H), 1.79–1.45 (m, 4H), 1.41 (s, 9H), 1.41–1.17 (m, 6H). $m/z = 472$ [$M + H$] $^+$.

Bz-Orn(N-Boc)-Ala-OEt (112). General procedure F was followed using Cbz-Orn(N-Boc)-Ala-OEt **58** (300 mg, 0.64 mmol) and benzoyl chloride (82 μ L, 0.70 mmol) to obtain **112** as a white solid (190 mg, 69%). ¹H NMR (CDCl₃): δ 7.83–7.48 (m, 2H), 7.48–7.34 (m, 5H), 5.03 (br s, 1H), 4.93 (br s, 1H), 4.51–4.46 (m, 1H), 4.22–4.12 (m, 2H), 3.35–3.05 (m, 2H), 2.04–1.78 (m, 2H), 1.69–1.60 (m, 2H), 1.41 (s, 9H), 1.36 (d, 3H, J 7.3 Hz), 1.26 (t, 3H, J 7.1 Hz). $m/z = 436$ [$M + H$] $^+$.

BzIOAc-Orn(N-Boc)-Ala-OEt (113). General procedure F was followed using Cbz-Orn(N-Boc)-Ala-OEt **58** (300 mg, 0.64 mmol) and benzyloxycarbonyl chloride (107 μ L, 0.70 mmol) to obtain **113** as a colorless oil (235 mg, 77%). ¹H NMR (CDCl₃): δ 7.40–7.30 (m, 5H), 7.23 (d, 1H, J 8.46 Hz), 7.02 (d, 1H, J 6.3 Hz), 4.82 (br s, 1H), 4.71–4.48 (m, 4H), 4.23–4.15 (m, 2H), 4.04–3.93 (m, 2H), 3.35–3.05 (m, 2H), 1.95–1.89 (m, 1H), 1.69–1.52 (m, 3H), 1.44–1.40 (m, 12H), 1.28 (t, 3H, J 7.2 Hz). $m/z = 480$ [$M + H$] $^+$.

PhCH₂SO₂-Orn(N-Boc)-Ala-OEt (114). General procedure F was followed using Cbz-Orn(N-Boc)-Ala-OEt **58** (300 mg, 0.64 mmol) and benzyloxycarbonyl chloride (143 mg, 0.70 mmol) to obtain **114** as a white solid (190 mg, 62%). ¹H NMR (CDCl₃): δ 7.44–7.34 (m, 5H), 7.02 (d, 1H, J 6.7 Hz), 5.55 (d, 1H, J 8.6 Hz), 4.89 (br s, 1H), 4.54–4.44 (m, 1H), 4.31–4.09 (m, 4H), 4.00 (br s, 1H), 3.25–2.95 (m, 2H), 1.80–1.43 (m, 16H), 1.25 (t, 3H, J 7.1 Hz). $m/z = 486$ [$M + H$] $^+$.

Boc-Sta-NH(CH₂)₂Ph (115). General procedure C was followed using Boc-Sta-OH **3** (700 mg, 2.54 mmol) and phenethylamine (616 mg, 5.08 mmol) to obtain **115** as a solid (950 mg, 99%). ¹H NMR (600 MHz, CDCl₃): δ 7.31 (t, $J = 7.6$ Hz, 2H), 7.25–7.17 (m, 3H), 6.29 (s, 1H), 4.77 (d, $J = 9.5$ Hz, 1H), 3.97–3.88 (m, 1H), 3.58–3.47 (m, 3H), 2.83 (t, $J = 7.1$ Hz, 2H), 2.41 (dd, $J = 14.8, 9.2$ Hz, 1H), 2.25 (dd, $J = 14.9, 3.3$ Hz, 1H), 1.68–1.60 (m, 1H), 1.58–1.50 (m, 1H), 1.43 (s, 9H), 1.35–1.28 (m, 1H), 0.91 (dd, $J = 6.6, 3.3$ Hz, 6H). $m/z = 379$ [$M + H$] $^+$.

PhSO₂-Arg(N,N-diBoc)-Ala-Sta-NH(CH₂)₂Ph (117). General procedure A was followed using PhSO₂-Orn(N-Boc)-Ala-Sta-NH(CH₂)₂Ph **67** (50 mg, 0.07 mmol) to obtain **117** as a colorless oil (55 mg, 92%). ¹H NMR (CDCl₃) (rotamers): δ 8.45–8.25 (m, 1H), 7.94–7.89 (m, 2H), 7.61–7.50 (m, 3H), 7.30–7.15 (m, 6H), 6.80–6.65 (m, 2H), 4.40–4.28 (m, 1H), 4.05–3.65 (m, 3H), 3.55–3.40 (m, 2H), 3.30–3.05 (m, 2H), 2.83–2.75 (m, 2H), 2.40–2.25 (m, 2H), 1.30–1.25 (m, 28H), 0.93–0.89 (m, 6H). $m/z = 846$ [M] $^+$.

Bz-Arg(N,N-diBoc)-Ala-Sta-NH(CH₂)₂Ph (118). General procedure A was followed using Bz-Orn(N-Boc)-Ala-Sta-NH(CH₂)₂Ph **65** (50 mg, 0.08 mmol) to obtain **118** as a colorless oil (55 mg, 91%). ¹H NMR (CDCl₃) (rotamers): δ 7.87–7.12 (m, 11H), 6.85 (m, 1H), 6.65 (m, 1H), 5.05–4.90 (m, 1H), 4.75–4.65 (m, 1H), 4.55–4.35 (m, 1H), 4.05–3.90 (m, 2H), 3.55–3.10 (m, 4H), 2.85–2.71 (m, 2H), 2.35–2.28 (m, 2H), 1.95–1.30 (28H, m), 0.90–0.79 (m, 6H). $m/z = 810$ [M] $^+$.

BzIOAc-Arg(N,N-diBoc)-Ala-Sta-NH(CH₂)₂Ph (119). General procedure A was followed using BzIOAc-Orn(N-Boc)-Ala-Sta-NH(CH₂)₂Ph **66** (50 mg, 0.07 mmol) to obtain **119** as a colorless oil (45 mg, 75%). ¹H NMR (CDCl₃) (rotamers): δ 7.37–7.15 (10H, m), 7.05 (br s, 0.5H), 6.70–6.60 (m, 1H), 6.49–6.45 (m, 0.5H), 4.99–4.84 (m, 1H),

4.60–4.30 (m, 4H), 4.00–3.85 (m, 4H), 3.55–3.35 (m, 2H), 3.25–3.05 (m, 2H), 2.84–2.77 (m, 2H), 2.30–2.25 (m, 2H), 1.85–1.35 (m, 28H), 0.91–0.87 (m, 6H). $m/z = 854$ [M] $^+$.

PhCH₂SO₂-Arg(N,N-diBoc)-Ala-Sta-NH(CH₂)₂Ph (120). General procedure A was followed using PhCH₂SO₂-Orn(N-Boc)-Ala-Sta-NH(CH₂)₂Ph **68** (50 mg, 0.07 mmol) to obtain **120** as a colorless oil (50 mg, 84%). ¹H NMR (CDCl₃) (rotamers): δ 7.40–7.15 (m, 10H), 6.90–6.65 (m, 2H), 6.10–5.95 (m, 1H), 4.98–4.86 (m, 1H), 4.55–4.26 (m, 3H), 4.00–3.83 (m, 3H), 3.55–3.25 (m, 2H), 3.24–2.95 (m, 2H), 2.84–2.73 (m, 2H), 2.32–2.20 (m, 2H), 1.75–1.30 (m, 28H), 1.44–0.87 (m, 6H). $m/z = 860$ [M] $^+$.

Boc-hPhe-Ala-OEt (121). General procedure C was followed using Boc-hPhe-OH (500 mg, 1.79 mmol) and HCl·NH₂-Ala-OEt (330 mg, 2.15 mmol) to obtain **121** as a white solid (500 mg, 74%). ¹H NMR (CDCl₃): δ 7.32–7.18 (m, 10H), 6.51 (br s, 1H), 5.07 (br s, 1H), 4.60–4.51 (m, 1H), 4.19 (q, 2H, J 7.1 Hz), 4.12 (br s, 1H), 2.72 (t, 2H, J 7.9 Hz), 2.21–2.12 (m, 1H), 2.00–1.90 (m, 1H), 1.47 (s, 9H), 1.41 (d, 3H, J 7.2 Hz), 1.29 (t, 3H, J 7.1 Hz). $m/z = 266$ [M] $^+$.

Boc-hPhe-Ala-OH (122). General procedure C was followed using Boc-hPhe-Ala-OEt **121** (450 mg, 1.2 mmol) to obtain **122** as a colorless oil (400 mg, 96%). ¹H NMR (CDCl₃): δ 7.29–7.20 (m, 5H), 6.89 (br s, 1H), 5.28 (br s, 1H), 4.60–4.50 (m, 1H), 4.20–4.10 (m, 1H), 2.75–2.65 (m, 2H), 2.17–1.85 (m, 2H), 1.45–1.35 (m, 12H). $m/z = 351$ [$M + H$] $^+$.

Boc-hPhe-Ala-Sta-NHCyhex (123). General procedure C was followed using Boc-hPhe-Ala-OH **122** (100 mg, 0.29 mmol) and HCl·NH₂-Sta-Cyhex **6** (92 mg, 0.314 mmol) to obtain **123** as a white solid (140 mg, 83%). ¹H NMR (CDCl₃) (rotamers): δ 7.32–7.17 (m, 5H), 6.90 (br s, 0.5 H), 6.70–6.25 (m, 2.5H), 5.30 (br s, 0.5 H), 5.15 (br s, 0.5H), 4.47–4.34 (m, 1H), 4.15–3.90 (m, 3H), 3.80–3.65 (m, 1H), 2.72–2.66 (m, 2H), 2.40–1.10 (m, 25H), 0.92–0.87 (m, 6H). $m/z = 589$ [M] $^+$.

■ ASSOCIATED CONTENT

Supporting Information

Parallel chemistry experimental, compound evaluation data, and BACE1 and cathepsin D sequence alignment data. This material is available free of charge via the Internet at <http://pubs.acs.org>.

■ AUTHOR INFORMATION

Corresponding Author

*Phone: +61 3 9345 2718. E-mail: sleebs@wehi.edu.au. Address: The Walter and Eliza Hall Institute of Medical Research, 1G Royal Parade, Parkville 3052, Victoria, Australia.

Notes

The authors declare no competing financial interest.

■ ACKNOWLEDGMENTS

This work was funded by the National Health and Medical Research Council of Australia (project grant 1010326 to J.A.B.), the Human Frontiers Science Program (RGY0073/2012 to J.A.B.), the Ramaciotti Foundation (establishment grant 3197/2010 to J.A.B.), a CASS Foundation Science and Medicine grant (SM.12.4348 to J.A.B.), the Australian Cancer Research Foundation, and a Victorian State Government Operational Infrastructure Support and Australian Government NHMRC IRIISS. We thank the University of Melbourne for the provision of a postgraduate scholarship awarded to M.G. A.F.C. is a Howard Hughes International Scholar and an Australia Fellow of the NHMRC. J.A.B. is a QEII Fellow of the Australian Research Council. We thank Dr Guillaume Lessene and Prof. David Huang for their helpful discussions.

■ ABBREVIATIONS USED

PMV, plasmepsin V; PEXEL, *Plasmodium* export element; Pf, *Plasmodium falciparum*; Pv, *Plasmodium vivax*; BACE-1, β -secretase-1; KAHRP, knob associated histidine rich protein; PfEMP3, *P. falciparum* erythrocyte membrane protein 3; PTEX, *Plasmodium* translocon of exported proteins; ER, endoplasmic reticulum; GFP, green fluorescent protein; PMVHA, immuno precipitated plasmepsin V tagged with 3x hemagglutinin tags; Cyhex, cyclohexyl; HBTU, *O*-(benzotriazol-1-yl)-*N,N,N',N'*-tetramethyluronium hexafluorophosphate; TFA, trifluoroacetic acid; CDI, *N,N'*-carbonyldiimidazole; AHMHpA, Boc-(3*S*,4*S*,5*S*)-4-amino-3-hydroxy-5-methylheptanoic acid; AHMHxA, (3*S*,4*S*)-4-amino-3-hydroxy-5-methylhexanoic acid; AHPPA, (3*S*,4*S*)-4-amino-3-hydroxy-5-phenylpentanoic acid; ACHPA, (3*S*,4*S*)-4-amino-3-hydroxy-5-cyclohexylpentanoic acid; Sta, (3*S*,4*S*)-4-amino-3-hydroxy-6-methylheptanoic acid; BzLOAc, benzyloxyacetyl; DCHA, *N,N*-dicyclohexylamine

■ REFERENCES

- (1) World Malaria Report; World Health Organization: Geneva, 2013; http://www.who.int/malaria/publications/world_malaria_report_2013/en/.
- (2) Mendis, K.; J, S. B.; P, M.; Carter, R. The neglected burden of *Plasmodium vivax* malaria. *Am. J. Trop. Med. Hyg.* **2001**, *64*, 97–106.
- (3) Marti, M.; Good, R. T.; Rug, M.; Knuefer, E.; Cowman, A. F. Targeting malaria virulence and remodeling proteins to the host erythrocyte. *Science* **2004**, *306*, 1930–1933.
- (4) Hiller, N. L.; Bhattacharjee, S.; van Ooij, C.; Liolios, K.; Harrison, T.; Lopez-Estrano, C.; Halder, K. A host-targeting signal in virulence proteins reveals a secretome in malarial infection. *Science* **2004**, *306*, 1934–1937.
- (5) Boddey, J. A.; Carvalho, T. G.; Hodder, A. N.; Sargeant, T. J.; Sleebbs, B. E.; Marapana, D.; Lopaticki, S.; Nebl, T.; Cowman, A. F. Role of Plasmepsin V in export of diverse protein families in the *Plasmodium falciparum* exportome. *Traffic* **2013**, *14*, 532–550.
- (6) Sargeant, T. J.; Marti, M.; Caler, E.; Carlton, J. M.; Simpson, K.; Speed, T. P.; Cowman, A. F. Lineage-specific expansion of proteins exported to erythrocytes in malaria parasites. *Genome Biol.* **2006**, *7*, R12.
- (7) Maier, A. G.; Rug, M.; O'Neill, M. T.; Brown, M.; Chakravorty, S.; Szesztak, T.; Chesson, J.; Wu, Y.; Hughes, K.; Coppel, R. L.; Newbold, C.; Beeson, J. G.; Craig, A.; Crabb, B. S.; Cowman, A. F. Exported proteins required for virulence and rigidity of *Plasmodium falciparum*-infected human erythrocytes. *Cell* **2008**, *134*, 48–61.
- (8) Chang, H. H.; Falick, A. M.; Carlton, P. M.; Sedat, J. W.; DeRisi, J. L.; Marletta, M. A. N-Terminal processing of proteins exported by malaria parasites. *Mol. Biochem. Parasitol.* **2008**, *160*, 107–115.
- (9) Boddey, J. A.; Moritz, R. L.; Simpson, R. J.; Cowman, A. F. Role of the *Plasmodium* export element in trafficking parasite proteins to the infected erythrocyte. *Traffic* **2009**, *10*, 285–299.
- (10) Russo, I.; Babbitt, S.; Muralidharan, V.; Butler, T.; Oksman, A.; Goldberg, D. E. Plasmepsin V licenses *Plasmodium* proteins for export into the host erythrocyte. *Nature* **2010**, *463*, 632–636.
- (11) Sleebbs, B. E.; Lopaticki, S.; Marapana, D. S.; O'Neil, M.; Rajasekaran, P.; Gazdik, M.; Günther, S.; Whitehead, L. W.; Lowes, K. N.; Barford, L.; Hviid, L.; Shaw, P. J.; Hodder, A. N.; Smith, B. J.; Cowman, A. F.; Boddey, J. A. Inhibition of plasmepsin V activity demonstrates its essential role in protein export, PfEMP1 display and survival of malaria parasites. *PLoS Biol.* **2014**, *12*, e1001897.
- (12) Akinyi, S.; Hanssen, E.; Meyer, E. V. S.; Jiang, J.; Korir, C. C.; Singh, B.; Lapp, S.; Barnwell, J. W.; Tilley, L.; Galinski, M. R. A 95 kDa protein of *Plasmodium vivax* and *P. cynomolgi* visualized by three-dimensional tomography in the caveola-vesicle complexes (Schüffner's dots) of infected erythrocytes is a member of the PHIST family. *Mol. Microbiol.* **2012**, *84*, 816–831.
- (13) Boddey, J. A.; Hodder, A. N.; Gunther, S.; Gilson, P. R.; Patsiouras, H.; Kapp, E. A.; Pearce, J. A.; de Koning-Ward, T. F.; Simpson, R. J.; Crabb, B. S.; Cowman, A. F. An aspartyl protease directs malaria effector proteins to the host cell. *Nature* **2010**, *463*, 627–631.
- (14) Klemba, M.; Goldberg, D. E. Characterization of plasmepsin V, a membrane-bound aspartic protease homolog in the endoplasmic reticulum of *Plasmodium falciparum*. *Mol. Biochem. Parasitol.* **2005**, *143*, 183–191.
- (15) Kappe, S. H.; Vaughan, A. M.; Boddey, J. A.; Cowman, A. F. That was then but this is now: malaria research in the time of an eradication agenda. *Science* **2010**, *328*, 862–866.
- (16) Eisenstein, M. Drug development: Holding out for reinforcements. *Nature* **2012**, *484*, S16–S18.
- (17) Johansson, P.-O.; Chen, Y.; Belfrage, A. K.; Blackman, M. J.; Kvarnström, I.; Jansson, K.; Vrang, L.; Hamelink, E.; Hallberg, A.; Rosenquist, Å.; Samuelsson, B. Design and synthesis of potent inhibitors of the malaria aspartyl proteases plasmepsin I and II. Use of solid-phase synthesis to explore novel statine motifs. *J. Med. Chem.* **2004**, *47*, 3353–3366.
- (18) Johansson, P.-O.; Lindberg, J.; Blackman, M. J.; Kvarnström, I.; Vrang, L.; Hamelink, E.; Hallberg, A.; Rosenquist, Å.; Samuelsson, B. Design and synthesis of potent inhibitors of plasmepsin I and II: X-ray crystal structure of inhibitor in complex with plasmepsin II. *J. Med. Chem.* **2005**, *48*, 4400–4409.
- (19) Nöteberg, D.; Hamelink, E.; Hultén, J.; Wahlgren, M.; Vrang, L.; Samuelsson, B.; Hallberg, A. Design and synthesis of plasmepsin I and plasmepsin II inhibitors with activity in *Plasmodium falciparum*-infected cultured human erythrocytes. *J. Med. Chem.* **2003**, *46*, 734–746.
- (20) Nöteberg, D.; Schaal, W.; Hamelink, E.; Vrang, L.; Larhed, M. High-speed optimization of inhibitors of the malarial proteases plasmepsin I and II. *J. Comb. Chem.* **2003**, *5*, 456–464.
- (21) Bonilla, J. A.; Bonilla, T. D.; Yowell, C. A.; Fujioka, H.; Dame, J. B. Critical roles for the digestive vacuole plasmepsins of *Plasmodium falciparum* in vacuolar function. *Mol. Microbiol.* **2007**, *65*, 64–75.
- (22) Eder, J.; Hommel, U.; Cumin, F.; Martoglio, B.; Gerhartz, B. Aspartic proteases in drug discovery. *Curr. Pharm. Des.* **2007**, *13*, 271–285.
- (23) Abbenante, G.; Fairlie, D. P. Protease inhibitors in the clinic. *Med. Chem.* **2005**, *1*, 71–104.
- (24) Drag, M.; Salvesen, G. S. Emerging principles in protease-based drug discovery. *Nature Rev. Drug Discovery* **2010**, *9*, 690–701.
- (25) Eder, J.; Hommel, U.; Cumin, F.; Martoglio, B.; Gerhartz, B. Aspartic proteases in drug discovery. *Curr. Pharm. Des.* **2007**, *13*, 271–285.
- (26) Baxter, E. W.; Conway, K. A.; Kennis, L.; Bischoff, F.; Mercken, M. H.; De Winter, H. L.; Reynolds, C. H.; Tounge, B. A.; Luo, C.; Scott, M. K.; Huang, Y.; Braeken, M.; Pieters, S. M. A.; Berthelot, D. J. C.; Masure, S.; Bruinzeel, W. D.; Jordan, A. D.; Parker, M. H.; Boyd, R. E.; Qu, J.; Alexander, R. S.; Brenneman, D. E.; Reitz, A. B. 2-Amino-3,4-dihydroquinazolines as inhibitors of BACE-1 (beta-site APP cleaving enzyme): use of structure based design to convert a micromolar hit into a nanomolar lead. *J. Med. Chem.* **2007**, *50*, 4261–4264.
- (27) Malamas, M. S.; Barnes, K.; Johnson, M.; Hui, Y.; Zhou, P.; Turner, J.; Hu, Y.; Wagner, E.; Fan, K.; Chopra, R.; Olland, A.; Bard, J.; Pangalos, M.; Reinhart, P.; Robichaud, A. J. Di-substituted pyridinyl aminohydantoins as potent and highly selective human beta-secretase (BACE1) inhibitors. *Bioorg. Med. Chem.* **2010**, *18*, 630–639.
- (28) Porcari, V.; Magnoni, L.; Terstappen, G. C.; Fecke, W. A continuous time-resolved fluorescence assay for identification of BACE1 inhibitors. *Assay Drug Dev. Technol.* **2005**, *3*, 287–297.
- (29) Yasuda, Y.; Kageyama, T.; Akamine, A.; Shibata, M.; Kominami, E.; Uchiyama, Y.; Yamamoto, K. Characterization of new fluorogenic substrates for the rapid and sensitive assay of cathepsin E and cathepsin D. *J. Biochem.* **1999**, *125*, 1137–1143.
- (30) Straub, A.; Roehrig, S.; Hillisch, A. Oral, direct thrombin and factor Xa inhibitors: the replacement for warfarin, leeches, and pig intestines? *Angew. Chem., Int. Ed.* **2011**, *50*, 4574–4590.

- (31) Rawlings, N. D.; Barrett, A. J.; Bateman, A. MEROPS: the database of proteolytic enzymes, their substrates and inhibitors. *Nucleic Acids Res.* **2012**, *40*, D343–D350.
- (32) Mastan, B. S.; Kumari, A.; Gupta, D.; Mishra, S.; Kumar, K. A. Gene disruption reveals a dispensable role for plasmepsin VII in the *Plasmodium berghei* life cycle. *Mol. Biochem. Parasitol.* **2014**, *195*, 10–13.
- (33) Coombs, G. H.; Goldberg, D. E.; Klemba, M.; Berry, C.; Kay, J.; Mottram, J. C. Aspartic proteases of *Plasmodium falciparum* and other parasitic protozoa as drug targets. *Trends Parasitol.* **2001**, *17*, 532–537.
- (34) Šali, A.; Blundell, T. L. Comparative protein modelling by satisfaction of spatial restraints. *J. Mol. Biol.* **1993**, *234*, 779–815.
- (35) Prade, L.; Jones, A. F.; Boss, C.; Richard-Bildstein, S.; Meyer, S.; Binkert, C.; Bur, D. X-ray structure of plasmepsin II complexed with a potent achiral inhibitor. *J. Biol. Chem.* **2005**, *280*, 23837–23843.
- (36) Bernstein, N. K.; Cherney, M. M.; Yowell, C. A.; Dame, J. B.; James, M. N. Structural insights into the activation of *P. vivax* plasmepsin. *J. Mol. Biol.* **2003**, *329*, 505–524.
- (37) Clarke, B.; Demont, E.; Dingwall, C.; Dunsdon, R.; Faller, A.; Hawkins, J.; Hussain, I.; MacPherson, D.; Maile, G.; Matico, R.; Milner, P.; Mosley, J.; Naylor, A.; O'Brien, A.; Redshaw, S.; Riddell, D.; Rowland, P.; Soleil, V.; Smith, K. J.; Stanway, S.; Stemp, G.; Sweitzer, S.; Theobald, P.; Vesey, D.; Walter, D. S.; Ward, J.; Wayne, G. BACE-1 inhibitors part 2: identification of hydroxy ethylamines (HEAs) with reduced peptidic character. *Bioorg. Med. Chem. Lett.* **2008**, *18*, 1017–1021.
- (38) Behnen, J.; Koster, H.; Neudert, G.; Craan, T.; Heine, A.; Klebe, G. Experimental and computational active site mapping as a starting point to fragment-based lead discovery. *ChemMedChem* **2012**, *7*, 248–261.
- (39) Hess, B.; Kutzner, C.; van der Spoel, D.; Lindahl, E. GROMACS 4: algorithms for highly efficient, load-balanced, and scalable molecular simulation. *J. Chem. Theory Comput.* **2008**, *4*, 435–437.
- (40) Jorgensen, W. L.; Tirado-Rives, J. The OPLS force field for proteins. Energy minimizations for crystals of cyclic peptides and crambin. *J. Am. Chem. Soc.* **1998**, *110*, 1657–1666.
- (41) Bussi, G.; Donadio, D.; Parrinello, M. Canonical sampling through velocity rescaling. *J. Chem. Phys.* **2007**, *126*, 014101.
- (42) Essman, U.; Perera, L.; Berkowitz, M. L.; Darden, T.; Lee, H.; Pedersen, L. G. A smooth particle mesh Ewald method. *J. Chem. Phys.* **1995**, *103*, 8577–92.
- (43) Hess, B. P-LINCS: a parallel linear constraint solver for molecular simulation. *J. Chem. Theory Comput.* **2008**, *4*, 116–122.
- (44) Gamo, F.-J.; Sanz, L. M.; Vidal, J.; de Cozar, C.; Alvarez, E.; Lavandera, J.-L.; Vanderwall, D. E.; Green, D. V. S.; Kumar, V.; Hasan, S.; Brown, J. R.; Peishoff, C. E.; Cardon, L. R.; Garcia-Bustos, J. F. Thousands of chemical starting points for antimalarial lead identification. *Nature* **2010**, *465*, 305–310.
- (45) Calculator Plugins were used for structure property prediction and calculation, Marvin 14.7.7.0, 2014, ChemAxon (<http://www.chemaxon.com>).